NASA TECHNICAL MEMORANDUM

NASA TM X-2590

NASA TM X-2590

EXAMINATION OF TWO METHODS OF DESCRIBING THE THERMODYNAMIC PROPERTIES OF OXYGEN NEAR THE CRITICAL POINT

by Thomas H. Rees and John T. Suttles

Langley Research Center
Hampton, Va. 23365

NATIONAL AERONAUTICS AND SPACE ADMINISTRATION • WASHINGTON, D. C. • SEPTEMBER 1972

1. Report No. NASA TM X-2590	2. Government Accession No.	3. Recipient's Catalog No.
4. Title and Subtitle EXAMINATION OF TWO METHODS OF DESCRIBING THE THERMODYNAMIC PROPERTIES OF OXYGEN NEAR THE CRITICAL POINT		5. Report Date September 1972 6. Performing Organization Code
7. Author(s) Thomas H. Rees and John T. Suttles		8. Performing Organization Report No. L-8418
9. Performing Organization Name and Address NASA Langley Research Center Hampton, Va. 23365		10. Work Unit No. 114-08-13-06 11. Contract or Grant No.
12. Sponsoring Agency Name and Address National Aeronautics and Space Administration Washington, D.C. 20546		13. Type of Report and Period Covered Technical Memorandum 14. Sponsoring Agency Code
15. Supplementary Notes		

16. Abstract

A computer study was conducted to compare the numerical behavior of two approaches to describing the thermodynamic properties of oxygen near the critical point. One approach utilized properties from the tabulated data presented by L. A. Weber, and the other approach was based on computing properties using the curve-fit equations developed by R. B. Stewart. Data on the relative differences between values of specific heats at constant pressure (c_p), density, and isotherm and isochor derivatives of the equation of state are presented for selected supercritical pressures at temperatures in the range 100 to 300 K. The results of a more detailed study of the c_p representations afforded by the two methods are also presented.

The correlation of the two methods at the selected pressures was very good outside the near-critical temperature region (150 to 170 K). Large differences (up to 30 percent) occurred within this region, however. The detailed study of c_p representations illustrated that these large discrepancies were due not to differences in the basic data of the methods but to the fact that the resolution of Weber's data in the near-critical region was not adequate to allow sufficient description of the thermodynamic functions by linear interpolation. In order to illustrate the effects of this poor description, identical calculations were performed based on the two methods of obtaining thermodynamic properties. Regions of erratic behavior in the calculations based on Weber's tabulations were correlated to errors introduced by linear interpolation.

17. Key Words (Suggested by Author(s))	18. Distribution Statement
Thermodynamic properties Cryogenic oxygen Oxygen	Unclassified – Unlimited

19. Security Classif. (of this report)	20. Security Classif. (of this page)	21. No. of Pages	22. Price*
Unclassified	Unclassified	37	$3.00

*For sale by the National Technical Information Service, Springfield, Virginia 22151

EXAMINATION OF TWO METHODS OF DESCRIBING THE THERMODYNAMIC PROPERTIES OF OXYGEN NEAR THE CRITICAL POINT

By Thomas H. Rees and John T. Suttles
Langley Research Center

SUMMARY

A computer study was conducted to compare the numerical behavior of two approaches to describing the thermodynamic properties of oxygen near the critical point. One approach utilized properties from the tabulated data presented by L. A. Weber, and the other approach was based on computing properties using the curve-fit equations developed by R. B. Stewart. Data on the relative differences between values of specific heats at constant pressure (c_p), density, and isotherm and isochor derivatives of the equation of state are presented for selected supercritical pressures at temperatures in the range 100 to 300 K. The results of a more detailed study of the c_p representations afforded by the two methods are also presented.

The correlation of the two methods at the selected pressures was very good outside the near-critical temperature region (150 to 170 K). Large differences (up to 30 percent) occurred within this region, however. The detailed study of c_p representations illustrated that these large discrepancies were due not to differences in the basic data of the methods but to the fact that the resolution of Weber's data in the near-critical region was not adequate to allow sufficient description of the thermodynamic functions by linear interpolation. In order to illustrate the effects of this poor description, identical calculations were performed based on the two methods of obtaining thermodynamic properties. Regions of erratic behavior in the calculations based on Weber's tabulations were correlated to errors introduced by linear interpolation.

INTRODUCTION

The removal of the mixing fans from the supercritical oxygen storage tanks in the Apollo spacecraft introduced the possibility that the fluid in the tank could be stratified, possibly giving rise to several serious effects. First, it could cause erroneous quantity probe measurements with the potential for precipitating a mission abort. Second, if the low-density fluid from the stratified layer entered the oxygen supply lines, the potential would exist for fuel-cell shutdown. Finally, if the stratified layer became too extensive,

a perturbing force of even extremely low magnitude could cause depressurization with the potential for the existence of two-phase fluid in the tank.

The concern about the effects of stratification in the redesigned tanks led to a significant volume of analytical study in that area (refs. 1, 2, and 3). The thermodynamic data for oxygen that served as bases for the various studies were not identical; some investigators used the tabulated data presented by L. A. Weber (ref. 4), while some relied on the curve-fit equations developed by R. B. Stewart (ref. 5).

Comparisons of results presented in references 1 to 3 with unpublished calculations made by J. T. Suttles and G. L. Smith of the Langley Research Center have revealed significant differences. For example, Suttles and Smith using Weber's tabulations for the thermodynamic data predict the generation of very rapid oscillations of the mean pressure in the tank (about 25 cycles per hour after 2 hours) for a high-density case whereas Baldwin, Reinhardt, and Sheaffer (ref. 1, ch. 6) using Stewart's equations predict rates of about $3\frac{1}{2}$ cycles per hour. Although the overall methods of analysis in the cited papers are diverse and thus undoubtedly contribute to the varying results, the contributions to these differences caused by the use of different descriptions of the thermodynamic data were also questioned. The purpose of this paper is, therefore, to compare the descriptions of the thermodynamic data for supercritical oxygen afforded by the two methods mentioned (refs. 4 and 5) and to compare the results of identical calculations based upon the two methods.

The approach taken was first to compute by each method values of specific heats at constant pressure (c_p), density, and the isotherm and isochor derivatives of the equation of state for supercritical pressures of 58.5 and 60 atm over the temperature range 100 to 300 K. The percent differences of values computed by Stewart's equations from interpolated values of Weber's tabulations were computed and plotted against temperature. The values of c_p were also plotted along selected isobars and isotherms. Finally, thermodynamic properties computed by Stewart's equations were applied to a simple mathematical model of the Apollo cryogenic oxygen storage tank for which the results of calculations based on Weber's tabulations were available.

SYMBOLS

A_i coefficients in vapor-pressure curve fit (eq. (4)), defined in appendix B, table IIIB

C_i coefficients in zero-pressure specific-heat equation (eq. (B3)), defined in appendix B, table IIB

c_p	specific heat at constant pressure, J/kg-K
c_p^o	specific heat at zero pressure, liter-atm/mole-K
$c_p(T)$	c_p as a function of T only, that is, along an isobar
f_i	functions for evaluating derivatives of equation of state (eq. 1)), defined in appendix A, table IVA
g_i	functions for evaluating integrals of thermodynamic equations, defined in appendix B, table IB
H	enthalpy, liter-atm/mole
$H^o_{T_o}$	reference enthalpy at triple point, liter-atm/mole
$\dot{m}$	mass flux, kg/hr
n_i	coefficients in Stewart's curve fit to equation of state for oxygen (eq. (1)), defined in appendix A, table IA
p	pressure, atm (1 atm = 101.325 kN/m^2)
p_V	vapor pressure, atm
R	characteristic gas constant for oxygen, 0.0820535 liter-atm/mole-K
T	temperature, K
T_c	temperature at critical point, K
T_o	temperature at triple point, K
t	time, sec
U	internal energy, liter-atm/mole
Q	heat flux, watts

X_i	functions for evaluating equation of state and derivatives, defined in appendix A
Y_i	functions for evaluating integrals of thermodynamic equations, defined in appendix B
ρ	density, mole/liter
ρ_c	critical density, mole/liter
ρ_{sat_L}	saturated liquid density, mole/liter
ρ_{sat_V}	saturated vapor density, mole/liter
$\left(\frac{\partial p}{\partial T}\right)_\rho$	isochor derivative of equation of state
$\left(\frac{\partial p}{\partial \rho}\right)_T$	isotherm derivative of equation of state

Subscripts:

COND	conduction
HTR	heater
input	input
leak	leak
net	net
RAD	radiation

METHOD

Two methods of describing the thermodynamic properties of oxygen were utilized in the present investigation. The first method was based on the least-squares curve fit to the equation of state for oxygen developed by Stewart (ref. 5). Stewart's curve fit gives pressure in terms of temperature and density over the entire range of data avail-

able at the time. The estimated accuracies of the equation of state over the three main temperature-pressure ranges are given as follows:

1. Gaseous range of values (65 to 300 K, to 340 atm) – ±0.1 percent in ρ
2. Liquid range (65 K to T_c, to 340 atm) – ±0.15 percent in ρ
3. Near-critical range (125 to 165 K, 40 to 100 atm) – ±0.3 percent in ρ

Stewart also presented methods for calculating entropy, enthalpy, internal energies, and specific heats from derived functions using his equation of state and its derivatives.

The second method of describing the thermodynamic properties of oxygen utilized in the present investigation involved interpolation of Weber's tabulations of the thermodynamic properties (ref. 4). Values of molar volume, isotherm and isochor derivatives of the equation of state, enthalpy, entropy, specific heats, and velocity of sound were tabulated as functions of pressure (to 330 atm) and temperature (T_o to 300 K). These data were presented in increments of 5 atm and 2 K up to 160 K and in increments of 5 atm and 5 K above 160 K.

For the purpose of the present study, values of c_p, ρ, $\left(\frac{\partial p}{\partial \rho}\right)_T$, and $\left(\frac{\partial p}{\partial T}\right)_\rho$ were taken directly from Weber's tabulations (ref. 4), read into the digital computer, and referenced by linear interpolation.

The equations required for utilization of Stewart's method were adapted from reference 5. The equations and procedures used in the present investigation are presented in detail. Also, a computer listing of subroutines used for applying Stewart's method is included as appendix C.

Equation of State

The curve fits for the thermodynamic properties of oxygen developed by Stewart (ref. 5) were programed into the computer. The least-squares curve fit for the equation of state, given in reference 5 as equation (7), is presented here as equation (1):

$$p = \rho RT + \left(n_1 T + n_2 + \frac{n_3}{T^2} + \frac{n_4}{T^4} + \frac{n_5}{T^6}\right)\rho^2 + \left(n_6 T^2 + n_7 T + n_8 + \frac{n_9}{T} + \frac{n_{10}}{T^2}\right)\rho^3$$

$$+ \left(n_{11} T + n_{12}\right)\rho^4 + \left(n_{13} + \frac{n_{14}}{T}\right)\rho^5 + \rho^3\left(\frac{n_{15}}{T^2} + \frac{n_{16}}{T^3} + \frac{n_{17}}{T^4}\right)\exp\left(n_{25}\rho^2\right)$$

$$+ \rho^5\left(\frac{n_{18}}{T^2} + \frac{n_{19}}{T^3} + \frac{n_{20}}{T^4}\right)\exp\left(n_{25}\rho^2\right) + \rho^7\left(\frac{n_{21}}{T^2} + \frac{n_{22}}{T^3} + \frac{n_{23}}{T^4}\right)\exp\left(n_{25}\rho^2\right)$$

$$+ n_{24}\rho^{n_{28}+1}\left(\rho^{n_{28}} - \rho_c^{n_{28}}\right)\exp\left[n_{26}\left(\rho^{n_{28}} - \rho_c^{n_{28}}\right)^2 + n_{27}\left(T - T_c\right)^2\right] \qquad (1)$$

The coefficients for equation (1), n_1 through n_{28}, are included in table IA of appendix A. The constraints for the critical point and the fixed-point data imposed by Stewart upon the curve fit for the equation of state are listed in tables IIA and IIIA of appendix A, respectively.

Since the calculations required density as a function of temperature and pressure, equation (1) was solved numerically for density by an iterative method.

The isochor derivative $\left(\frac{\partial p}{\partial T}\right)_\rho$ and the isotherm derivative $\left(\frac{\partial p}{\partial \rho}\right)_T$ of equation (1) are given in appendix A as equations (A2) and (A3), respectively.

Specific Heat Calculations

Since the method of Stewart (ref. 5) does not include a procedure for calculating c_p throughout the entire range of supercritical conditions being considered, it was necessary to adopt the procedure described in this section. The approach is based upon the use of the enthalpy equation to produce a consistent calculation of c_p for the entire range of interest.

The specific heat at constant pressure was approximated by a central differencing of the enthalpy versus temperature curve;

$$c_p(T,\rho) = \frac{H(T + \Delta T,\rho_1) - H(T - \Delta T,\rho_2)}{2\,\Delta T} \tag{2}$$

where ρ_1 and ρ_2 are densities at $T + \Delta T$ and $T - \Delta T$, respectively, for a given pressure. A temperature increment $\Delta T = 1.0$ K was used in equation (2), except in the near-critical region (150 K $\leqq T \leqq$ 170 K) where $\Delta T = 0.1$ K was used to improve the approximation. A brief computer study showed that, for $\Delta T = 0.1$ K, a halving of the temperature increment to $\Delta T = 0.05$ K produced a change in c_p of less than 0.2 percent in the near-critical region, which is within the accuracy of Stewart's curve-fit equations.

Using the method of reference 5, it was necessary to calculate the enthalpies for equation (2) differently for temperatures above and below T_c. The procedure is described in the following sections.

Temperatures above critical.- For temperatures above T_c the enthalpy used in equation (2) was calculated by equation (18) of reference 5, given here as equation (3)

$$H(T,\rho) = H^o_{T_o} + T\int_0^\rho \left[\frac{R}{\rho} - \frac{1}{\rho^2}\left(\frac{\partial p}{\partial T}\right)_\rho\right]_T d\rho + \int_0^\rho \left(\frac{p}{\rho^2} - \frac{RT}{\rho}\right)_T d\rho$$

$$+ \frac{p - \rho RT}{\rho} + \int_{T_o}^{T} c_p^o\, dT \tag{3}$$

The solution to the integrals over ρ in equation (3) is simplified by using the equation of state (eq. (1)) and its isochor derivative (eq. (A2)). The indefinite solutions to the three integrals in equation (3) are given in appendix B. The reference enthalpy used was the enthalpy of the ideal gas at the triple point $T_o = 55.0$ K which is $H^o_{T_o} = 15.7$ liter-atm/mole (ref. 5).

Temperatures below critical.- The method used for calculation of the enthalpy of supercritical oxygen at temperatures below T_c involved integration of internal energies from the saturation point along an isotherm. The use of internal energies in this region is part of the method of reference 5. The sequence of computations is described as follows:

First, the vapor pressure was calculated from the vapor-pressure curve fit for oxygen given as equation (7) in reference 4,

$$\log_e p_V(T) = A_1 + A_2T + A_3T^2 + A_4T^3 + A_5T^4 + A_6T^5 + A_7T^6 + A_8T^7 \tag{4}$$

The A_i's for equation (4) are listed in table IIIB of appendix B.

Next, the saturated liquid and vapor densities, ρ_{sat_L} and ρ_{sat_V}, were calculated by the simultaneous solution of the equation of state (eq. (1)) and the vapor-pressure curve (eq. (4)).

The saturated-vapor enthalpies were calculated by evaluating equation (3) at T, ρ_{sat_V}, and p_V. The saturated-liquid enthalpies were calculated by subtracting the enthalpy change due to vaporization as given by the Clapeyron equation from the saturated-vapor enthalpy:

$$H\left(T,\rho_{sat_L}\right) = H\left(T,\rho_{sat_V}\right) - T\left(\frac{dp_V}{dT}\right)\left(\frac{1}{\rho_{sat_V}} - \frac{1}{\rho_{sat_L}}\right) \tag{5}$$

where $\left(\frac{dp_V}{dT}\right)$ is the derivative of the vapor-pressure curve (eq. (4)).

The internal energies and the enthalpies were related as follows:

$$U(T,\rho) = H(T,\rho) - \frac{p}{\rho} \tag{6}$$

The internal energies were calculated by equation (24) of reference 5, given here as follows:

$$U(T,\rho) = U\left(T,\rho_{sat_L}\right) - T\int_{\rho_{sat_L}}^{\rho}\left[\frac{1}{\rho^2}\left(\frac{\partial p}{\partial T}\right)_\rho\right]_T d\rho + \int_{\rho_{sat_L}}^{\rho}\frac{p}{\rho^2}\,d\rho \tag{7}$$

where $U\left(T,\rho_{sat_L}\right)$ is the saturated-liquid internal energy, calculated from equations (5) and (6). The solutions to the integrals in equation (7) were facilitated by the use of the following relations:

$$-\int\left[\frac{1}{\rho^2}\left(\frac{\partial p}{\partial T}\right)_\rho\right]_T d\rho = \int\left[\frac{R}{\rho} - \frac{1}{\rho^2}\left(\frac{\partial p}{\partial T}\right)_\rho\right]_T d\rho - R \log_e \rho \tag{8}$$

$$\int \frac{p}{\rho^2} d\rho = \int\left(\frac{p}{\rho^2} - \frac{RT}{\rho}\right)_T d\rho + RT \log_e \rho \tag{9}$$

After the appropriate substitutions are made, equation (7) becomes

$$U(T,\rho) = U\left(T,\rho_{sat_L}\right) + T\int_{\rho_{sat_L}}^{\rho}\left[\frac{R}{\rho} - \frac{1}{\rho^2}\left(\frac{\partial p}{\partial T}\right)_\rho\right]_T d\rho + \int_{\rho_{sat_L}}^{\rho}\left(\frac{p}{\rho^2} - \frac{RT}{\rho}\right)_T d\rho \tag{10}$$

The integrals used in equation (10) are the same as those used in equation (3).

Finally, the enthalpy used in equation (2) was calculated by equation (6).

Numerical difficulties.- Iterating for the saturation densities was complicated by the existence of an extraneous positive real root of equation (1) which lies between the roots representing the saturated vapor and liquid densities. Calculation of the extraneous root was avoided by careful choice of the bounds on the iteration. Evaluation of equation (A3), the isotherm derivative of the equation of state, at each calculated root provided a check for extraneous roots, since the isotherm derivative is always positive at the saturation densities but negative at the extraneous root. The problem of the extraneous root to equation (1) is addressed more comprehensively by Walter A. Reinhardt in reference 1, chapter 4.

Discontinuities were calculated in the c_p-isobars at T_c. Since the temperature range encompassing the discontinuities was only about 2 K at the pressures investigated, this problem was circumvented by calculating c_p's above and below the discontinuity and interpolating linearly along the isobar for intermediate temperatures.

Stewart's equations (ref. 5) exhibited sensitivity to propagation of errors. The large number of operations involved tend to mushroom seemingly insignificant relative errors in ρ, for example, into large relative errors in p calculated from equation (1). This effect can be minimized by demanding higher-order accuracy on the iterations for ρ, and by programing for minimum propagation of errors. (Reduction of the number of computer operations is one effective method for minimizing propagated errors.) A discussion of computer propagation of errors may be found in a numerical-methods text such as reference 6.

The method described above for calculation of c_p's proved to be expensive in computer run time relative to a table look-up method; consequently, care was required in the coding and logical flow to insure maximum efficiency.

PROCEDURE

The procedure used in the present study involved first calculating values of c_p, ρ, $\left(\frac{\partial p}{\partial \rho}\right)_T$, and $\left(\frac{\partial p}{\partial T}\right)_\rho$ for two supercritical pressures (58.5 and 60 atm) and a range of temperatures, 100 to 300 K, in 2 K increments. The percent differences between values from Stewart's method and from Weber's tabulations were computed by the following relation:

$$\text{Percent difference} = \frac{\text{Stewart's value - Weber's value}}{\text{Weber's value}} \times 100$$

These percent differences were plotted against temperature in figure 1. Values of c_p were then calculated over the temperature range 130 to 180 K in increments of 0.2 K along the isobars 55, 60, and 58.5 atm and are presented as plots in figure 2. In figure 3, a family of similar curves from reference 4 is presented for comparison. Values of c_p were also calculated over a range of pressures, 55 to 70 atm, in increments of 1 atm for four isotherms, 140, 157, 160, and 180 K. These isotherms are presented as figure 4.

In order to explore the effects on calculated results caused by using Stewart's method rather than Weber's, identical calculations were performed and compared. In these calculations use was made of a simple mathematical model of the Apollo cryogenic oxygen storage tank developed by J. T. Suttles and G. L. Smith. Suttles and Smith used a one-dimensional cylindrical tank model as shown in figure 5 which facilitated a solution but retained the essential features of the actual tank. Their calculations gave the time rate of change of pressure as a function of temperature for two mass flux rates, 0.2268 kg/hr or 0.5 lb/hr and 0.6804 kg/hr or 1.5 lb/hr, both for heat addition $(Q_{net} = 125 \text{ watts})$ and for no heat addition. The present calculations were made for pressures of 58.5 and 60 atm. The 60-atm case shows comparison of the results based on the two thermodynamic representations at a pressure at which Weber's data were tabulated. The 58.5-atm case duplicates the conditions imposed on the calculations of Suttles and Smith. The results of the calculations are presented as plots in figure 6.

RESULTS AND DISCUSSION

Thermodynamic Properties

The percent differences in the thermodynamic properties calculated by the different methods (figs. 1(a) to 1(d)) range between zero and 3 percent outside the near-critical

region (150 K < T < 170 K); however, large differences were noted inside this region. Also, the error introduced by linear interpolation of Weber's tabulations appears to have a significant effect upon the percent differences. The magnitudes of the percent differences were, in general, larger at points representing interpolated Weber's data than at points representing tabulated data. The differences in c_p were by far the most significant; therefore, c_p was selected for a detailed examination.

Figures 2(a) to 2(c) present comparisons of values of c_p produced by the different methods plotted as functions of temperature along three isobars (55 atm, 60 atm, and 58.5 atm). It should again be noted that agreement outside the near-critical temperature region (150 K to 170 K) appears to be very good. Furthermore, the points corresponding to tabulated data in reference 4 (circled points, 55 and 60 atm) agree very well with values calculated by Stewart's curve fits over the entire temperature range; if the circled points were faired smoothly, the faired curves would closely approximate the curves calculated from Stewart's equations. This statement is supported by figure 3, which was taken directly from reference 4. Although the isobars from figure 2 do not appear in figure 3, the smoothness and characteristic shape of the 50- and 70-atm isobars of figure 3 give strong support to at least the shape of the c_p-curves obtained from Stewart's equations shown in figure 2.

Since figures 2(a) and 2(b) represent data at pressures at which values of c_p were tabulated in reference 4, the poor behavior of Weber's data in the proximity of the peaks could only be due to linear interpolation of $c_p(T)$ between points too widely spaced in temperature to describe the peak adequately. Figure 2(c), on the other hand, represents the 58.5-atm isobar, which is between tabulated pressures. This figure, therefore, illustrates the combined effect of double first-order interpolation of c_p, which appears to be only slightly worse than the effect of interpolating $c_p(T)$ along the tabulated isobars.

Figure 4, a comparison of c_p's along selected isotherms, is presented to illustrate better the effects of linear interpolation of pressure. The 140 and 180 K isotherms lie outside the near-critical region and reassert the statement that first-order interpolation of Weber's data is sufficient outside of this region. The 160 K isotherm (a tabulated temperature) illustrates the irregularity introduced by linear interpolation of c_p with pressure in regions where the slope of the curve changes rapidly. Although the relative accuracy of the two methods at points where tabulated data exist in reference 4 has not been established, certainly Stewart's equations yield smoother results in the near-critical region than linear interpolation of Weber's tabulated data. Finally, the 157 K isotherm again represents a comparison of the results of Stewart's method with double-interpolated Weber's data corresponding to the peak of figure 2(a). The greatest part of the deviation of this pair of curves near 55 atm is attributed to interpolation of c_p with temperature since 55 atm is a tabulated pressure. The error caused by first-order

interpolation of c_p with pressure appears to be relatively insignificant compared to the gross error caused by first-order interpolation of the $c_p(T)$-curves near their peaks.

Calculations for Tank With Uniform Properties

The calculations for a uniform tank performed by Suttles and Smith were repeated, and the results are presented in figures 6(a) and 6(b). The calculations gave the time rate of change of pressure as a function of temperature for two mass flux rates, 0.2268 kg/hr or 0.5 lb/hr and 0.6804 kg/hr or 1.5 lb/hr, both for heat addition (Q_{net} = 125 watts) and for no heat addition. The calculations were made using both methods for description of the thermodynamic properties of oxygen for two pressures (p = 60 atm and 58.5 atm). Results from the two methods agreed over the entire temperature range for no heat addition, and for temperatures greater than 170 K for the heat-addition case. The methods also agreed fairly well for the latter case up to approximately 140 K. The divergent behavior between 140 and 154 K correlates with differences in the thermodynamic properties previously noted in that range.

The relative behavior of the results based upon the two methods in the region between 154 and 170 K warrants special attention, however. The results from Weber's data in figure 6(a) up to 160 K correspond to tabulated thermodynamic properties from reference 4. It is important to note that the pressure derivatives calculated from Weber's data at 162 and 164 K correspond to regions of poor description of the peak in the $c_p(T)$-curve by linear interpolation (figs. 2(b) and 2(c)), while the derivatives at 58.5 atm, 156 and 158 K, correspond to points of large percent differences in all the thermodynamic properties (fig. 1).

In summary, comparison of figures 6(a) and 6(b) indicates that the variations in the pressure derivative between 154 and 170 K calculated from linearly interpolated data from reference 4 (these variations were described as "unusual" by Suttles and Smith) were caused by the error introduced by such interpolation.

The calculations for the stratified-tank problem performed by Suttles and Smith were not made, but significant differences in the behavior of calculations around the critical temperature could be expected.

CONCLUDING REMARKS

A study was made to compare the approximations of the thermodynamic behavior of supercritical oxygen as afforded by Weber's tabulations and by Stewart's curve-fit equations as presented in this paper. Comparisons were presented for density, the isotherm and isochor derivatives of the equation of state, and specific heat at constant pressure (c_p) for a range of temperatures and two supercritical pressures. Special attention was

given to approximations of c_p. Calculations for a simple one-dimensional mathematical model of the redesigned Apollo cryogenic oxygen storage tank with uniform properties were made based upon both approximations of the thermodynamic properties of oxygen. The results were plotted and presented for comparison.

In general, the thermodynamic properties obtained by the two methods agreed very well except in the near-critical temperature region (150 to 170 K). Stewart's equations were more effective in approximating the general shapes of the curves of the thermodynamic properties in regions of rapid variation than linear interpolation of Weber's tabulations. The resolution of Weber's data was insufficient for first-order interpolation in regions of rapid variation in the thermodynamic properties. Additional tabulated data near the critical point would greatly enhance the reliability of Weber's tabulations in this region.

Similarly, the results of the uniform-tank calculations agreed for temperatures above 170 K. Regions of erratic numerical behavior in the results of the calculations based on Weber's tabulations were correlated to errors introduced by linear interpolation.

From a utilization standpoint, both methods of describing the thermodynamic properties of oxygen have advantages. For limited ranges of temperature and pressures such as those in the present study, the table look-up method was considered more convenient and efficient for computer programing. On the other hand, if a very wide range of conditions must be studied, the large number of data points required for this method could make computer storage requirements the limiting factor; the curve-fit method becomes more advantageous as the ranges of temperature and pressure increase.

If Stewart's equations are to be employed, certain obvious techniques can be incorporated to enhance the efficiency of the method; for instance, the problem should be formulated so that temperature and density are the independent variables. Owing to the large number of operations involved, calculation of specific heats should be avoided if possible, especially in the near-critical region where the uncertainty of the representation is the greatest. Stewart's equations should be programed to avoid redundant operations and to minimize propagation of errors.

More recent data are now available (refs. 7 and 8) which improve the description of the thermodynamic behavior of oxygen in the critical region; nevertheless, linear interpolation in this region is not recommended. Regardless of the methods of describing thermodynamic properties chosen for future investigations, a brief numerical study of the description afforded will probably disclose any gross misrepresentations of the data similar to linear interpolation of Weber's tabulations in the critical region.

Langley Research Center,
National Aeronautics and Space Administration,
Hampton, Va., July 25, 1972.

APPENDIX A

DERIVATIVES OF THE EQUATION OF STATE (REF. 5)

Equation of State

The equation of state (eq. (1)) may be written

$$p = \rho RT + \sum_{i=1}^{24} n_i X_i \tag{A1}$$

where the n_i's are the coefficients listed in table IA, and the X_i functions are as follows:

$X_1 = \rho^2 T$	$X_9 = \rho^3/T$	$X_{17} = \rho^3 f_1/T^4$
$X_2 = \rho^2$	$X_{10} = \rho^3/T^2$	$X_{18} = \rho^5 f_1/T^2$
$X_3 = \rho^2/T^2$	$X_{11} = \rho^4 T$	$X_{19} = \rho^5 f_1/T^3$
$X_4 = \rho^2/T^4$	$X_{12} = \rho^4$	$X_{20} = \rho^5 f_1/T^4$
$X_5 = \rho^2/T^6$	$X_{13} = \rho^5$	$X_{21} = \rho^7 f_1/T^2$
$X_6 = \rho^3 T^2$	$X_{14} = \rho^5/T$	$X_{22} = \rho^7 f_1/T^3$
$X_7 = \rho^3 T$	$X_{15} = \rho^3 f_1/T^2$	$X_{23} = \rho^7 f_1/T^4$
$X_8 = \rho^3$	$X_{16} = \rho^3 f_1/T^3$	$X_{24} = \rho^{(n_{28}+1)} f_2 f_3$

The f_1's are given in table IVA.

Isochor Derivative

The isochor derivative $\left(\frac{\partial p}{\partial T}\right)_\rho$ for equation (A1) is given as

$$\left(\frac{\partial p}{\partial T}\right)_\rho = \rho R + \sum_{i=1}^{24} n_i X_i \tag{A2}$$

where the n_i's are the coefficients listed in table IA, and the X_i functions are as follows:

$X_1 = \rho^2$ $\quad X_9 = -\rho^3/T^2$ $\quad X_{17} = -4\rho^3 f_1/T^5$

$X_2 = 0$ $\quad X_{10} = -2\rho^3/T^3$ $\quad X_{18} = -2\rho^5 f_1/T^3$

$X_3 = -2\rho^2/T^3$ $\quad X_{11} = \rho^4$ $\quad X_{19} = -3\rho^5 f_1/T^4$

$X_4 = -4\rho^2/T^5$ $\quad X_{12} = 0$ $\quad X_{20} = -4\rho^5 f_1/T^5$

$X_5 = -6\rho^2/T^7$ $\quad X_{13} = 0$ $\quad X_{21} = -2\rho^7 f_1/T^3$

$X_6 = 2T\rho^3$ $\quad X_{14} = -\rho^5/T^2$ $\quad X_{22} = -3\rho^7 f_1/T^4$

$X_7 = \rho^3$ $\quad X_{15} = -2\rho^3 f_1/T^3$ $\quad X_{23} = -4\rho^7 f_1/T^5$

$X_8 = 0$ $\quad X_{16} = -3\rho^3 f_1/T^4$ $\quad X_{24} = \rho^{(n_{28}+1)} f_2 f_4$

The f_i's are given in table IVA.

Isotherm Derivative

The isotherm derivative $\left(\frac{\partial p}{\partial \rho}\right)_T$ for equation (A1) is given by

$$\left(\frac{\partial p}{\partial \rho}\right)_T = RT + \sum_{i=1}^{24} n_i X_i \tag{A3}$$

where the n_i's are the coefficients listed in table IA, and the X_i functions are as follows:

$X_1 = 2\rho T$ $\quad X_9 = 3\rho^2/T$ $\quad X_{17} = f_6/T^4$

$X_2 = 2\rho$ $\quad X_{10} = 3\rho^2/T^2$ $\quad X_{18} = f_7/T^2$

$X_3 = 2\rho/T^2$ $\quad X_{11} = 4\rho^3 T$ $\quad X_{19} = f_7/T^3$

$X_4 = 2\rho/T^4$ $\quad X_{12} = 4\rho^3$ $\quad X_{20} = f_7/T^4$

$X_5 = 2\rho/T^6$ $\quad X_{13} = 5\rho^4$ $\quad X_{21} = f_8/T^2$

$X_6 = 3\rho^2 T^2$ $\quad X_{14} = 5\rho^4/T$ $\quad X_{22} = f_8/T^3$

$X_7 = 3\rho^2 T$ $\quad X_{15} = f_6/T^2$ $\quad X_{23} = f_8/T^4$

$X_8 = 3\rho^2$ $\quad X_{16} = f_6/T^3$ $\quad X_{24} = f_9 f_2 f_3 + \rho^{(n_{28}+1)} f_{10} f_3 + \rho^{(n_{28}+1)} f_2 f_{11}$

The f_i's are given in table IVA.

TABLE IA.- COEFFICIENTS FOR EQUATION (1)

T in K, p in atm, ρ in mole/liter		
R = 0.0820535	$n_{10} = -3.59419602 \times 10$	$n_{19} = -2.67817667 \times 10^{2}$
$n_1 = 3.38759078 \times 10^{-3}$	$n_{11} = 1.02209557 \times 10^{-6}$	$n_{20} = 1.05670904 \times 10^{5}$
$n_2 = -1.31606223$	$n_{12} = 1.90454505 \times 10^{-4}$	$n_{21} = 5.63771075 \times 10^{-3}$
$n_3 = -7.38828523 \times 10^{3}$	$n_{13} = 1.21708394 \times 10^{-5}$	$n_{22} = -1.12012813$
$n_4 = 1.92049067 \times 10^{7}$	$n_{14} = 2.44255945 \times 10^{-3}$	$n_{23} = 1.46829491 \times 10^{2}$
$n_5 = -2.90260005 \times 10^{10}$	$n_{15} = 1.73655508 \times 10^{2}$	$n_{24} = 9.98868924 \times 10^{-4}$
$n_6 = -5.70101162 \times 10^{-8}$	$n_{16} = 3.01752841 \times 10^{5}$	$n_{25} = -0.00560$
$n_7 = 7.96822375 \times 10^{-5}$	$n_{17} = -3.49528517 \times 10^{7}$	$n_{26} = -0.157$
$n_8 = 6.07022502 \times 10^{-3}$	$n_{18} = 8.86724004 \times 10^{-1}$	$n_{27} = -0.350$
$n_9 = -2.71019658$		$n_{28} = 0.90$

TABLE IIA.- CONSTRAINTS IMPOSED ON EQUATION (1)

p,ρ,T at the critical point	$\begin{cases} p = 50.14 \text{ atm} \\ \rho = 13.333 \text{ mole/liter} \\ T = 154.77 \text{ K} \end{cases}$
$\left(\frac{\partial p}{\partial \rho}\right)_T = 0$ at the critical point	
$\left(\frac{\partial^2 p}{\partial \rho^2}\right)_T = 0$ at the critical point	
$\left(\frac{\partial p}{\partial T}\right)_\rho = 1.928386$ atm/K at the critical point	

TABLE IIIA.- FIXED-POINT DATA

Critical pressure	50.14 atm
Critical temperature	154.77 K
Critical density	13.333 mole/liter
Normal boiling temperature (International practical temperature scale (IPTS), fixed point)	90.18 K
Density saturated vapor at normal boiling point (eq. (1))	0.1396 mole/liter
Density saturated liquid at normal boiling point (eq. (1))	35.65 mole/liter
Triple point pressure	0.00150 atm
Triple point temperature	54.353 K

TABLE IVA.- FUNCTIONS FOR EVALUATING DERIVATIVES OF EQUATION OF STATE

$f_1 = \exp\left(n_{25}\rho^2\right)$

$f_2 = \rho^{n_{28}} - \rho_c{}^{n_{28}}$

$f_3 = \exp\left[n_{26}f_2{}^2 + n_{27}(T - T_c)^2\right]$

$f_4 = 2n_{27}(T - T_c)f_3$

$f_5 = 2f_1\rho n_{25}$

$f_6 = 3f_1\rho^2 + f_5\rho^3$

$f_7 = 5f_1\rho^4 + f_5\rho^5$

$f_8 = 7f_1\rho^6 + f_5\rho^7$

$f_9 = (n_{28} + 1)\rho^{n_{28}}$

$f_{10} = n_{28}\rho^{(n_{28}-1)}$

$f_{11} = 2f_2n_{26}f_3f_{10}$

$f_{12} = 2f_5\rho n_{25} + 2f_1n_{25}$

$f_{13} = 6f_1\rho + 6f_5\rho^2 + f_{12}\rho^3$

$f_{14} = 20f_1\rho^3 + 10f_5\rho^4 + f_{12}\rho^5$

$f_{15} = 42f_1\rho^5 + 14f_5\rho^6 + f_{12}\rho^7$

$f_{16} = n_{28}(n_{28} + 1)\rho$

$f_{17} = n_{28}(n_{28} - 1)\rho^{(n_{28}-2)}$

$f_{18} = (2f_{10}n_{26}f_3 + 2f_2n_{26}f_{11})f_{10} + 2f_2n_{26}f_3f_{17}$

APPENDIX B

INTEGRATION OF THE THERMODYNAMIC EQUATIONS (REF. 5)

The solution of the integral $\int\left[\frac{R}{\rho} - \frac{1}{\rho^2}\left(\frac{\partial p}{\partial T}\right)_\rho\right]d\rho$ (from eq. (3)) at constant temperature is given by equation (B1). This integration uses the isochor derivative $\left(\frac{\partial p}{\partial T}\right)_\rho$ given in appendix A as equation (A2).

$$\int\left[\frac{R}{\rho} - \frac{1}{\rho^2}\left(\frac{\partial p}{\partial T}\right)_\rho\right]_T d\rho = \sum_{i=1}^{24} n_i Y_i \tag{B1}$$

where the n_i's are the coefficients listed in table IA, and the Y_i functions are as follows:

$Y_1 = -\rho$ $\quad$ $Y_9 = \rho^2/(2T^2)$ $\quad$ $Y_{17} = 4g_4/T^5$

$Y_2 = 0$ $\quad$ $Y_{10} = \rho^2/T^3$ $\quad$ $Y_{18} = 2g_5/T^3$

$Y_3 = 2\rho/T^3$ $\quad$ $Y_{11} = -\rho^3/3$ $\quad$ $Y_{19} = 3g_5/T^4$

$Y_4 = 4\rho/T^5$ $\quad$ $Y_{12} = 0$ $\quad$ $Y_{20} = 4g_5/T^5$

$Y_5 = 6\rho/T^7$ $\quad$ $Y_{13} = 0$ $\quad$ $Y_{21} = 2g_6/T^3$

$Y_6 = \rho^2 T$ $\quad$ $Y_{14} = \rho^4/(4T^2)$ $\quad$ $Y_{22} = 3g_6/T^4$

$Y_7 = -\rho^2/2$ $\quad$ $Y_{15} = 2g_4/T^3$ $\quad$ $Y_{23} = 4g_6/T^5$

$Y_8 = 0$ $\quad$ $Y_{16} = 3g_4/T^4$ $\quad$ $Y_{24} = -n_{27}(T - T_c)g_3/(n_{28}n_{26})$

where the g_i's are given in table IB.

The solution of the integral $\int\left(\frac{p}{\rho^2} - \frac{RT}{\rho}\right)d\rho$ at constant temperature is given by equation (B2). This integration uses $p = f(T,\rho)$ from equation of state (eq. (A1)) as given in appendix A.

$$\int\left(\frac{p}{\rho^2} - \frac{RT}{\rho}\right)_T d\rho = \sum_{i=1}^{24} n_i Y_i \tag{B2}$$

where the n_i's are the coefficients listed in table IA, and the Y_i functions are as follows:

$$Y_1 = T\rho \qquad Y_9 = \rho^2/(2T) \qquad Y_{17} = g_4/T^4$$

$$Y_2 = \rho \qquad Y_{10} = \rho^2/(2T^2) \qquad Y_{18} = g_5/T^2$$

$$Y_3 = \rho/T^2 \qquad Y_{11} = \rho^3 T/3 \qquad Y_{19} = g_5/T^3$$

$$Y_4 = \rho/T^4 \qquad Y_{12} = \rho^3/3 \qquad Y_{20} = g_5/T^4$$

$$Y_5 = \rho^2 T^6 \qquad Y_{13} = \rho^4/4 \qquad Y_{21} = g_6/T^2$$

$$Y_6 = \rho^2 T^2/2 \qquad Y_{14} = \rho^4/(4T) \qquad Y_{22} = g_6/T^3$$

$$Y_7 = \rho^2 T/2 \qquad Y_{15} = g_4/T^2 \qquad Y_{23} = g_6/T^4$$

$$Y_8 = \rho^2/2 \qquad Y_{16} = g_4/T^3 \qquad Y_{24} = g_3/(2n_{28}n_{26})$$

where the g_i's are given in table IB.

The solution of the integral $\int c_p^o \, dT$ is given by

$$\int c_p^o \, dT = R \sum_{i=1}^{8} C_i Y_i \tag{B3}$$

where R is given in table IA, and the C_i's are the coefficients listed in table IIB, and the Y_i functions are as follows:

$$Y_1 = -1/(2T^2) \qquad Y_5 = T^2/2$$

$$Y_2 = -1/T \qquad Y_6 = T^3/3$$

$$Y_3 = \log_e T \qquad Y_7 = T^4/4$$

$$Y_4 = T \qquad Y_8 = uT/(e^u - 1)$$

where $u = C_9/T$.

TABLE IB.- FUNCTIONS FOR EVALUATING INTEGRALS OF THERMODYNAMIC EQUATIONS

$$g_1 = \exp\left(n_{25}\rho^2\right)$$

$$g_2 = \rho^{n_{28}} - \rho_c^{n_{28}}$$

$$g_3 = \exp\left[n_{26}g_2^{\,2} + n_{27}(T - T_c)^2\right]$$

$$g_4 = g_1 \Big/ \left(2n_{25}\right)$$

$$g_5 = g_1\left(n_{25}\rho^2 - 1\right) \Big/ \left(2n_{25}^2\right)$$

$$g_6 = g_1\left[n_{25}^2\rho^4 - 2\left(n_{25}\rho^2 - 1\right)\right] \Big/ \left(2n_{25}^3\right)$$

TABLE IIB.- COEFFICIENTS FOR ZERO-PRESSURE SPECIFIC-HEAT EQUATION

$C_1 = -1.86442361 \times 10^{2}$	$C_6 = -1.11035799 \times 10^{-8}$
$C_2 = 2.07840241 \times 10$	$C_7 = 2.08612876 \times 10^{-11}$
$C_3 = -3.42642911 \times 10^{-1}$	$C_8 = 1.01894691$
$C_4 = 3.50297163$	$C_9 = 2.23918105 \times 10^{3}$
$C_5 = 2.05866482 \times 10^{-7}$	

TABLE IIIB.- COEFFICIENTS FOR VAPOR-PRESSURE EQUATION (EQ. 4)

T in K, p_V in atm, ρ in mole/liter
$A_1 = -62.5967185$
$A_2 = 2.47450429$
$A_3 = -4.68973315 \times 10^{-2}$
$A_4 = 5.48202337 \times 10^{-4}$
$A_5 = -4.09349868 \times 10^{-6}$
$A_6 = 1.91471914 \times 10^{-8}$
$A_7 = -5.13113688 \times 10^{-11}$
$A_8 = 6.02656934 \times 10^{-14}$

APPENDIX C

LISTING OF FORTRAN SUBROUTINES FOR STEWART'S METHOD

```
      SUBROUTINE STEWART(TEMP,RHO,PRESS,CP,DPDT,DPDRHO,ENERGY)
C     INPUT PRESS(ATM) RHO(GM-MOLE/L)
      DIMENSION XN(28)
      COMMON/N/XN,TEMPCR,RHOCRIT,R
      DATA(XN(I),I=1,28)/3.38759078E-3,-1.31606223,-7.38828523E+3,
     11.92049067E+7,-2.90260005E+10,-5.70101162E-8,7.96822375E-5,
     26.07022502E-3,-2.71019658,-3.59419602E+1,1.02209557E-6,
     31.90454505E-4,1.21708394E-5,2.44255945E-3,1.73655508E+2,
     43.01752841E+5,-3.49528517E+7,8.86724004E-1,-2.67817667E+2,
     51.05670904E+5,5.63771075E-3,-1.12012813,1.46829491E+2,
     69.98868924E-4,-.00560,-.157,-.350,.9/
      RHODUM=RHO
      PCRIT=50.14
      01=C1C2C4(TEMP,RHO)
      DPDT=C2(TEMP,RHO)*1.01325E+5
      DPDRHO=C4(TEMP,RHO)*1.01325E+5/31.9988
      CP=CPHU(TEMP,RHO,01    )*1.01325E+5/31.9988
      PRESS=01*1.01325E+5
      ENERGY=0.
      RHO=RHODUM
      RETURN
      END
```

```
      FUNCTION CPHU(TEMP,RHO,P)
C     ALL PRESSURES IN ATM  ALL DENSITIES IN GM-MOLE/L
C     CPHU(L-ATM/GM-MOLE/K)  H(L-ATM/GM-MOLE)  U,DITTO
      EXTERNAL FOFX
      COMMON/THERM/P1,T
      COMMON C1,C2
      DIMENSION A(8),H(2)
      DATA(A(I),I=1,8)/6.02656934E-14,-5.13113688E-11,1.91471914E-8,
     1-4.09349868E-6,5.48202337E-4,-4.68973315E-2,2.47450429,
     2-62.5967185/
      ENTHALP(T,RHO,RHO1,P)=1590.929*9.86896E-3+P/RHO-.0820535*T
     A-D5(55.,RHO)
     1-D2(T,RHO1)-D1D2D5(T,RHO1)*T+D5(T,RHO)+D2(T,RHO)+D1D2D5(T,RHO)*T
      ENERGY(T,RHO,RHO1,USAT)=USAT-D2(T,RHO1)-D1D2D5(T,RHO1)*T+D2(T,RHO)
     1+D1D2D5(T,RHO)*T
      R=0.0820535 $ RHODUM=RHO $ ICOUNT=0 $EREL=5.E-7 $ TINCR=1.0
      TI=153. $ TIP1=155.2
      IF(TEMP.GT.TI.AND.TEMP.LT.TIP1)GO TO 2222
      GO TO 1111
 2222 FACTOR=31.9988/1.01325E5
      CPI=C1*FACTOR
      CPIP1=C2*FACTOR
      CP=CPI+(TEMP-TI)/(TIP1-TI)*(CPIP1-CPI)
      CPHU=CP
      RETURN
 1111 IF(TEMP.GE.150..AND.TEMP.LE.170.)TINCR=0.1
      DELT=2.*TINCR
    6 IF(ICOUNT.EQ.2)GO TO 205
      T=TEMP-TINCR $ ICOUNT=ICOUNT+1 $ TINCR=-TINCR
      ASSIGN 1 TO INDEX
      NDEX=1
      P1=P
      RGM=.8*RHO$RGP=1.2*RHO$DELTRG=.1*RGM
      IF(T.GT.155..AND.T.LT.162.)RGM=.5*RHO
      EREL=5.E-7
      EABS=EREL*RGM
    9 CALL ITR2(RHO,RGM,RGP,DELTRG,FOFX,EREL, EABS,50,ICODE)
      IF(ICODE.NE.0)GO TO 1000
      GO TO INDEX,(1,55,60)
    1 IF(T.LT.154.77)GO TO 10
    5 H(ICOUNT)=ENTHALP(T,RHO,0.,P)
      GO TO 6
   10 PVLN=A(1)
      DO 15 I=2,8
   15 PVLN=PVLN*T+A(I)
      PV=EXP(PVLN)
      IF(P.LE.PV)GO TO 5
      RSAVE=RHO $ P1=PV
   59 RGM=4.*(EXP(0.0232*PV)-1.) $ RGP=RHO*.6$ DELTRG=.1*RGP-.1*RGM
      IF(T.GT.153.)EREL=5.E-10
      EABS=EREL*RGM
      NDEX=60
      ASSIGN 60 TO INDEX
      GO TO 9
   60 RSATV=RHO
      RGM=30.-1.5*RSATV $ RGP=1.1*RSAVE $ DELTRG=(RGP-RGM)*.2
      EABS=EREL*RGM
      NDEX=55
```

```
      ASSIGN 55 TO INDEX
      GO TO 9
   55 RSATL=RHO
   90 CONTINUE
      SUM=A(1)*7.
      DO 100 I=2,7
  100 SUM=SUM*T+(8-I)*A(I)
      DPVDT=SUM*PV
      DELTH=T*DPVDT*(1./RSATV-1./RSATL)
  150 HRSATV=ENTHALP(T,RSATV,0.,PV)
      HRSATL=HRSATV-DELTH
      USAT=HRSATL-PV/RSATL
      RHO=RSAVE
      U=ENERGY(T,RHO,RSATL,USAT)
      H(ICOUNT)=U+P/RHO
      GO TO 6
  205 CPHU=(H(2)-H(1))/DELT
      T1=TEMP-TINCR $ T2=TEMP+TINCR
  900 FORMAT(10X,*T1 = *,F8.3,*    T2 = * ,F8.3,*    H(T1) = *,E11.4,
     1 *    H(T2) = *,E11.4,*  RV,RL  *,2E11.4)
      RHO=RHODUM
      RETURN
 1000 WRITE(6,2)ICODE,NDEX
    2 FORMAT(1H0,21HERROR IN CPHU  ICODE=I2,5X,*INDEX = *,I2///)
      RETURN
      END
```

```
      FUNCTION C1C2C4(TEMP,RHO)
      DIMENSION X(24),XN(28),F(18)
      COMMON/N/XN,TEMPCR,RHOCRIT,R
      R=0.0820535
      RHOCRIT=13.333
      TEMPCR=154.77
      F(1)=EXP(XN(25)*RHO**2) $ F(2)=RHO**XN(28)-RHOCRIT**XN(28)
      F(3)=EXP(XN(26)*F(2)**2+XN(27)*(TEMP-TEMPCR)**2)
      X(1)=RHO**2*TEMP $ X(2)=RHO**2 $ X(3)=RHO**2/TEMP**2
      X(4)=RHO**2/TEMP**4 $ X(5)=RHO**2/TEMP**6 $ X(6)=RHO**3*TEMP**2
      X(7)=RHO**3*TEMP $ X(8)=RHO**3 $ X(9)=RHO**3/TEMP
      X(10)=RHO**3/TEMP**2 $ X(11)=RHO**4*TEMP $ X(12)=RHO**4
      X(13)=RHO**5 $ X(14)=RHO**5/TEMP $ X(15)=RHO**3*F(1)/TEMP**2
      X(16)=RHO**3*F(1)/TEMP**3 $ X(17)=RHO**3*F(1)/TEMP**4
      X(18)=RHO**5*F(1)/TEMP**2 $ X(19)=RHO**5*F(1)/TEMP**3
      X(20)=RHO**5*F(1)/TEMP**4 $ X(21)=RHO**7*F(1)/TEMP**2
      X(22)=RHO**7*F(1)/TEMP**3 $ X(23)=RHO**7*F(1)/TEMP**4
      X(24)=RHO**(XN(28)+1.)*F(2)*F(3)
      FACTOR=RHO*R*TEMP
      GO TO 10
      ENTRY C2
      F(4)=2.*XN(27)*(TEMP-TEMPCR)*F(3) $ F(5)=2.*F(1)*RHO*XN(25)
      X(1)=RHO**2 $ X(2)=0. $ X(3)=-2.*RHO**2/TEMP**3
      X(4)=-4.*RHO**2/TEMP**5 $ X(5)=-6.*RHO**2/TEMP**7
      X(6)=2.*TEMP*RHO**3 $ X(7)=RHO**3 $ X(8)=0. $ X(9)=-RHO**3/TEMP**2
      X(10)=-2.*RHO**3/TEMP**3 $ X(11)=RHO**4 $ X(12)=0. $ X(13)=0.
      X(14)=-RHO**5/TEMP**2 $ X(15)=-2.*RHO**3*F(1)/TEMP**3
      X(16)=-3.*RHO**3*F(1)/TEMP**4 $ X(17)=-4.*RHO**3*F(1)/TEMP**5
      X(18)=-2.*RHO**5*F(1)/TEMP**3 $ X(19)=-3.*RHO**5*F(1)/TEMP**4
      X(20)=-4.*RHO**5*F(1)/TEMP**5 $ X(21)=-2.*RHO**7*F(1)/TEMP**3
      X(22)=-3.*RHO**7*F(1)/TEMP**4 $ X(23)=-4.*RHO**7*F(1)/TEMP**5
      X(24)=RHO**(XN(28)+1.)*F(2)*F(4)
      FACTOR=RHO*R
      GO TO 10
      ENTRY C4
      F(6)=3.*F(1)*RHO**2+F(5)*RHO**3 $ F(7)=5.*F(1)*RHO**4+F(5)*RHO**5
      F(8)=7.*F(1)*RHO**6+F(5)*RHO**7 $ F(9)=(XN(28)+1.)*RHO**XN(28)
      F(10)=XN(28)*RHO**(XN(28)-1.) $ F(11)=2.*F(2)*XN(26)*F(3)*F(10)
      X(1)=2.*RHO*TEMP $ X(2)=2.*RHO $ X(3)=2.*RHO/TEMP**2
      X(4)=2.*RHO/TEMP**4 $ X(5)=2.*RHO/TEMP**6 $ X(6)=3.*RHO**2*TEMP**2
      X(7)=3.*RHO**2*TEMP $ X(8)=3.*RHO**2 $ X(9)=3.*RHO**2/TEMP
      X(10)=3.*RHO**2/TEMP**2 $ X(11)=4.*RHO**3*TEMP $ X(12)=4.*RHO**3
      X(13)=5.*RHO**4 $ X(14)=5.*RHO**4/TEMP $ X(15)=F(6)/TEMP**2
      X(16)=F(6)/TEMP**3 $ X(17)=F(6)/TEMP**4 $ X(18)=F(7)/TEMP**2
      X(19)=F(7)/TEMP**3 $ X(20)=F(7)/TEMP**4 $ X(21)=F(8)/TEMP**2
      X(22)=F(8)/TEMP**3 $ X(23)=F(8)/TEMP**4
      X(24)=F(9)*F(2)*F(3)+RHO**(XN(28)+1.)*F(10)*F(3)+RHO**(XN(28)+1.)*
     1F(2)*F(11)
      FACTOR=R*TEMP
   10 SUM=0.
      DO 1 I=1,24
    1 SUM=SUM+XN(I)*X(I)
      C1C2C4=SUM*FACTOR
      RETURN
      END
```

```
      FUNCTION D1D2D5(T,RHO)
      DIMENSION XN(28),G(6),Y(24),C(9)
      COMMON/N/XN,TCR,RHOCR,R
      DATA (C(I),I=1,9)/-1.86442361E+2,2.07840241E+1,-3.42642911E-1,
     13.50297163,2.05866482E-7,-1.11035799E-8,2.08612876E-11,
     21.01894691,2.23918105E+3/
      TEMPCR=TCR $ RHOCRIT=RHOCR$TEMP=T
      G(1)=EXP(XN(25)*RHO**2) $ G(2)=RHO**XN(28)-RHOCRIT**XN(28)
      G(4)=G(1)/(2.*XN(25))
      G(5)=G(1)*(XN(25)*RHO**2-1.)/(2.*XN(25)**2)
      G(6)=G(1)*(XN(25)**2*RHO**4-2.*(XN(25)*RHO**2-1.))/(2.*XN(25)**3)
      G(3)=EXP(XN(26)*G(2)**2+XN(27)*(TEMP-TEMPCR)**2)
      RHOSQ=RHO*RHO $ T2=T*T $ T3=T2*T $ T4=T3*T $ T5=T4*T
      Y(1)=-RHO $ Y(2)=0. $ Y(3)=2.*RHO/T3      $ Y(4)=4.*RHO/T5
      Y(5)=6.*RHO/T**7 $ Y(6)=RHOSQ*T $ Y(7)=-RHOSQ/2. $ Y(8)=0.
      Y(9)=RHOSQ/(2.*T2) $ Y(10)=RHOSQ/T3 $ Y(11)=-RHO**3/3.
      Y(12)=Y(13)=0. $ Y(14)=RHO**4/(4.*T2) $ Y(15)=2.*G(4)/T3
      Y(16)=3.*G(4)/T4 $ Y(17)=4.*G(4)/T5 $ Y(18)=2.*G(5)/T3
      Y(19)=3.*G(5)/T4 $ Y(20)=4.*G(5)/T5 $ Y(21)=2.*G(6)/T3
      Y(22)=3.*G(6)/T4 $ Y(23)=4.*G(6)/T5
      Y(24)=-XN(27)*(T-TCR)*G(3)/(XN(28)*XN(26))
      GO TO 10
      ENTRY D2
      RHO3=RHOSQ*RHO $ RHO4=RHO3*RHO
      Y(1)=T*RHO $ Y(2)=RHO $ Y(3)=RHO/T2 $ Y(4)=RHO/T4 $ Y(5)=RHO/T**6
      Y(6)=RHOSQ*T2/2. $ Y(7)=RHOSQ*T/2. $ Y(8)=RHOSQ/2.
      Y(9)=.5*RHOSQ/T $ Y(10)=.5*RHOSQ/T2 $ Y(11)=RHO3*T/3.
      Y(12)=RHO3/3. $ Y(13)=RHO4/4. $ Y(14)=.25*RHO4/T
      Y(15)=G(4)/T2 $ Y(16)=G(4)/T3 $ Y(17)=G(4)/T4
      Y(18)=G(5)/T2 $ Y(19)=G(5)/T3 $ Y(20)=G(5)/T4
      Y(21)=G(6)/T2 $ Y(22)=G(6)/T3 $ Y(23)=G(6)/T4
      Y(24)=G(3)/(2.*XN(28)*XN(26))
   10 SUM=0.
      DO 11 I=1,24
   11 SUM=SUM+Y(I)*XN(I)
      D1D2D5=SUM
      RETURN
      ENTRY D5
      U=C(9)/T $ T2=T*T $ T3=T2*T $ T4=T3*T
      Y(1)=-.5/T2 $ Y(2)=-1./T $ Y(3)=ALOG(T) $ Y(4)=T $ Y(5)=.5*T2
      Y(6)=T3/3. $ Y(7)=T4/4. $ Y(8)=U*T/(EXP(U)-1.)
      SUM=0.
      DO 20 I=1,8
   20 SUM=SUM+C(I)*Y(I)
      D1D2D5= SUM *R
      RETURN
      END
```

REFERENCES

1. Computational Fluid Dynamics Br., Ames Research Center: Convection in the Tanks of a Rotating Spacecraft. NASA TR R-386, 1972.

2. Saxton, J. A.: Two Fluid Model for Thermal Stratification in the Apollo Cryogenic Oxygen Tanks. TM-71-2031-2, Bellcomm, Inc., Oct. 22, 1971. (Available as NASA CR-124753.)

3. Heinmiller, P. J.: User's Manual for the GNAT Computer Program: Numerical Analysis of Stratification in Supercritical Oxygen. 17618-H121-R0-00 (Contract NAS 9-8166), TRW Systems Group, Mar. 1971. (Available as NASA CR-114963.)

4. Weber, L. A.: Thermodynamic and Related Properties of Oxygen From the Triple Point to 300 K at Pressures to 330 Atmospheres. NBS Rep. 9710, June 20, 1968. (Available as NASA CR-99159.)

5. Stewart, Richard Byron: The Thermodynamic Properties of Oxygen. PH. D. Diss., Univ. of Iowa, June 1966.

6. Stark, Peter A.: Introduction to Numerical Methods. Macmillan Co., c.1970.

7. Weber, L. A.: Density and Compressibility of Oxygen in the Critical Region. Phys. Rev. A, Third ser., vol. 2, no. 6, Dec. 1970, pp. 2379-2388.

8. McCarty, Robert D.; and Weber, Lloyd A.: Thermophysical Properties of Oxygen From the Freezing Liquid Line to 600 R for Pressures to 5000 psia. NBS Tech. Note 384, July 1971. (Available as NASA CR-121739.)

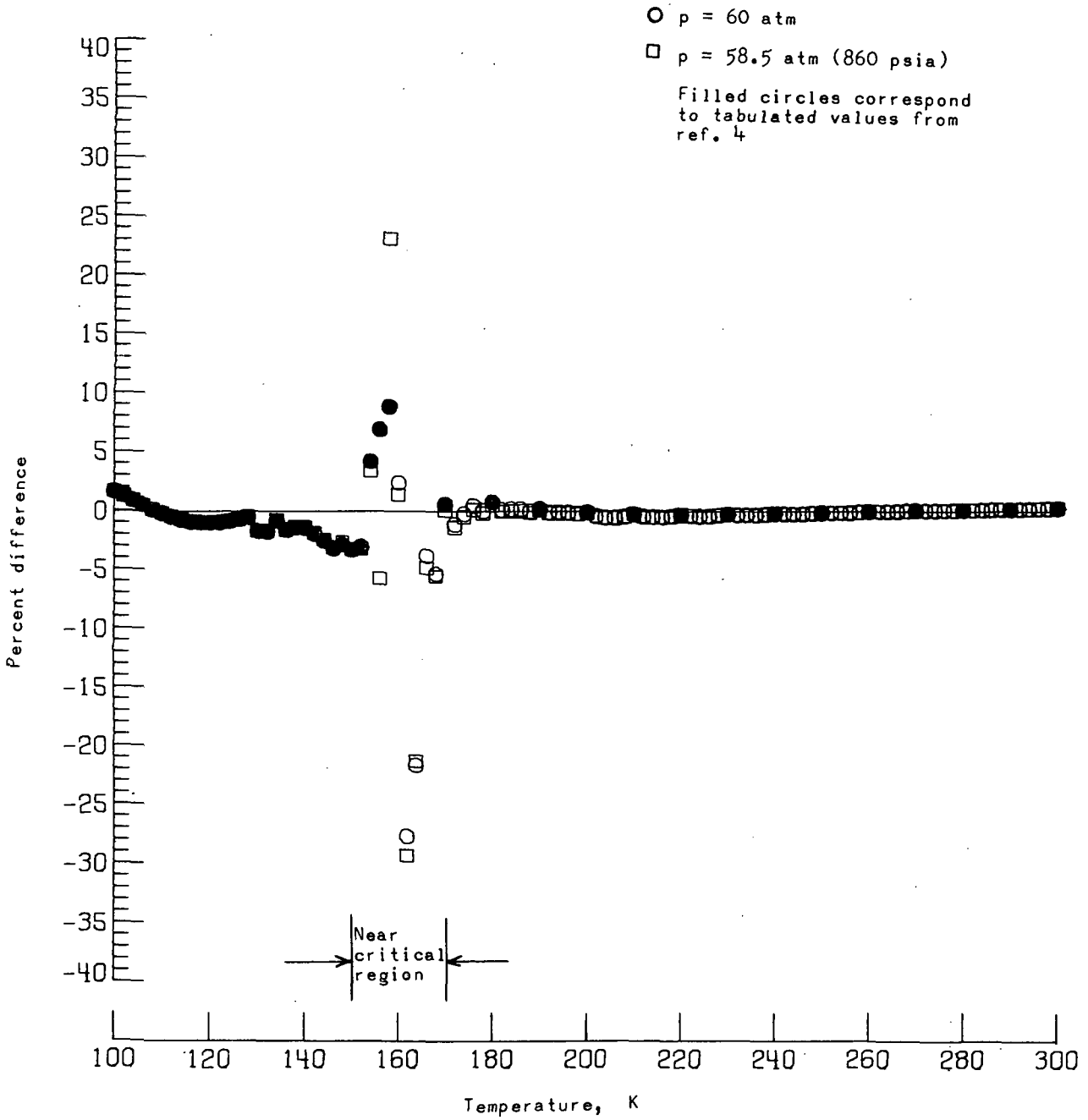

(a) Specific heat c_p.

Figure 1.- Percent difference between values of thermodynamic properties calculated by Stewart's method and values from interpolation (Weber's tabulations). Percent differences given by

$$\frac{\text{Stewart's value - Weber's value}}{\text{Weber's value}} \times 100$$

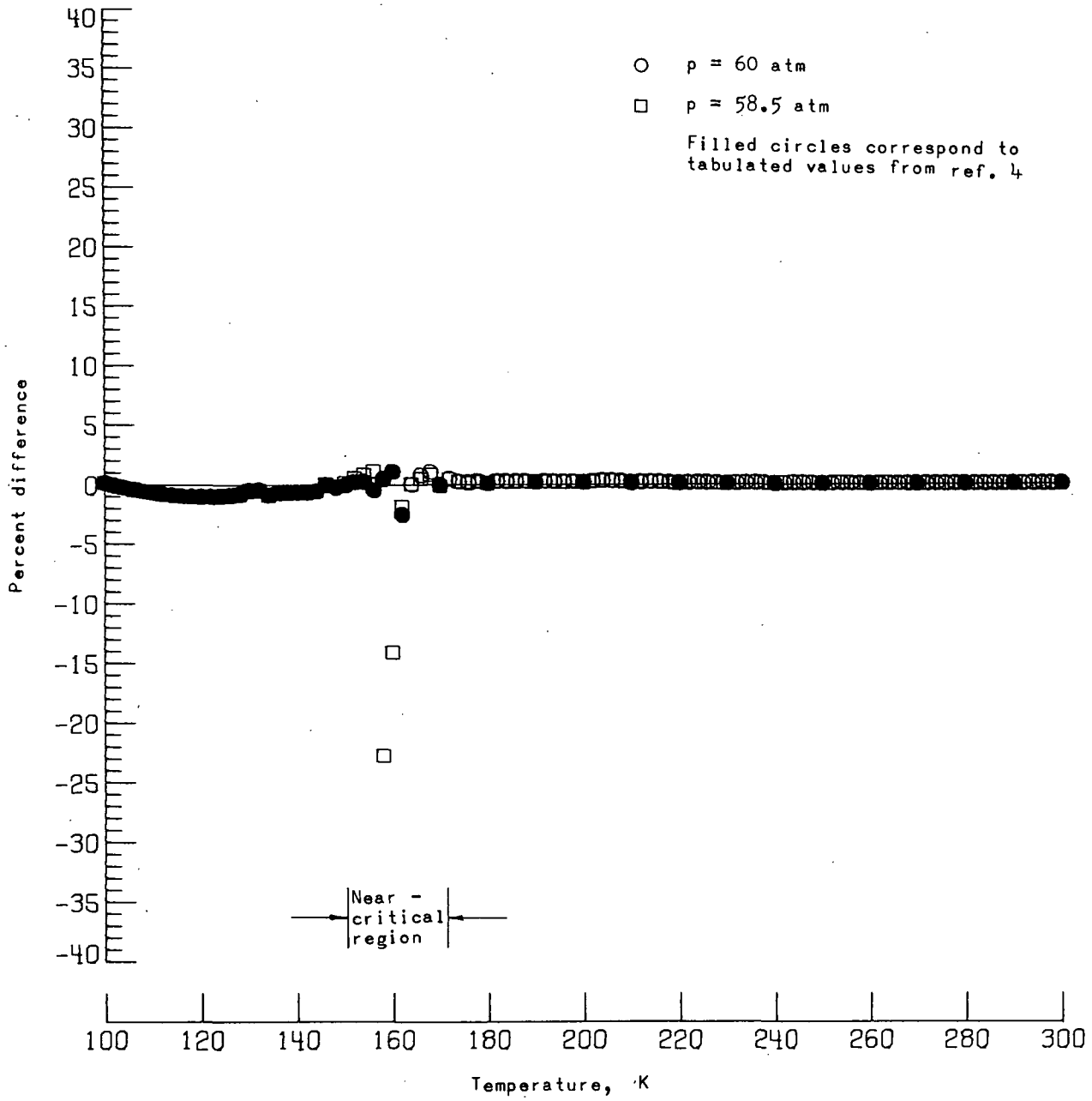

(b) Density ρ.

Figure 1.- Continued.

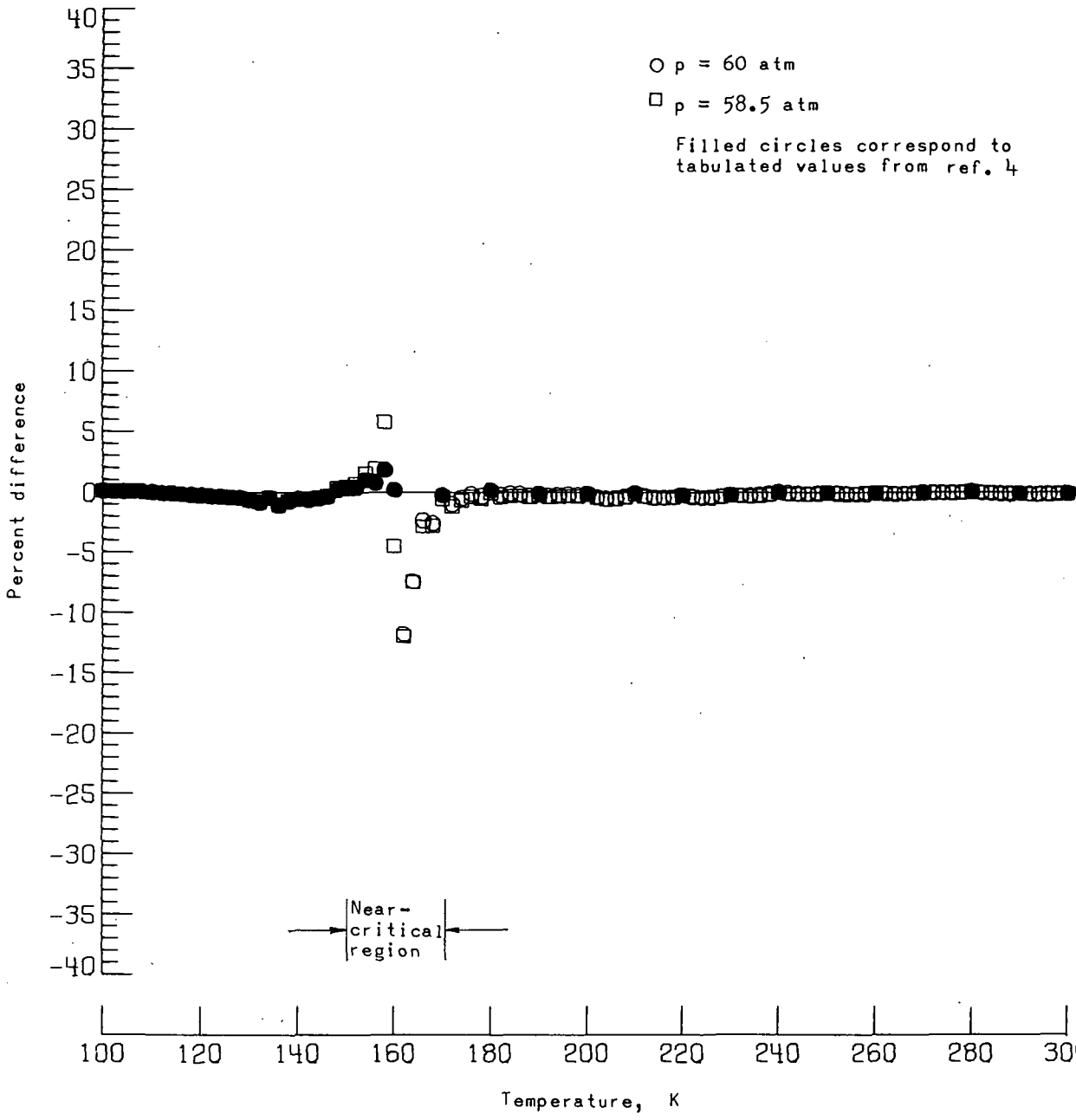

(c) Isochor derivative $\left(\frac{\partial p}{\partial T}\right)_{\rho}$.

Figure 1.- Continued.

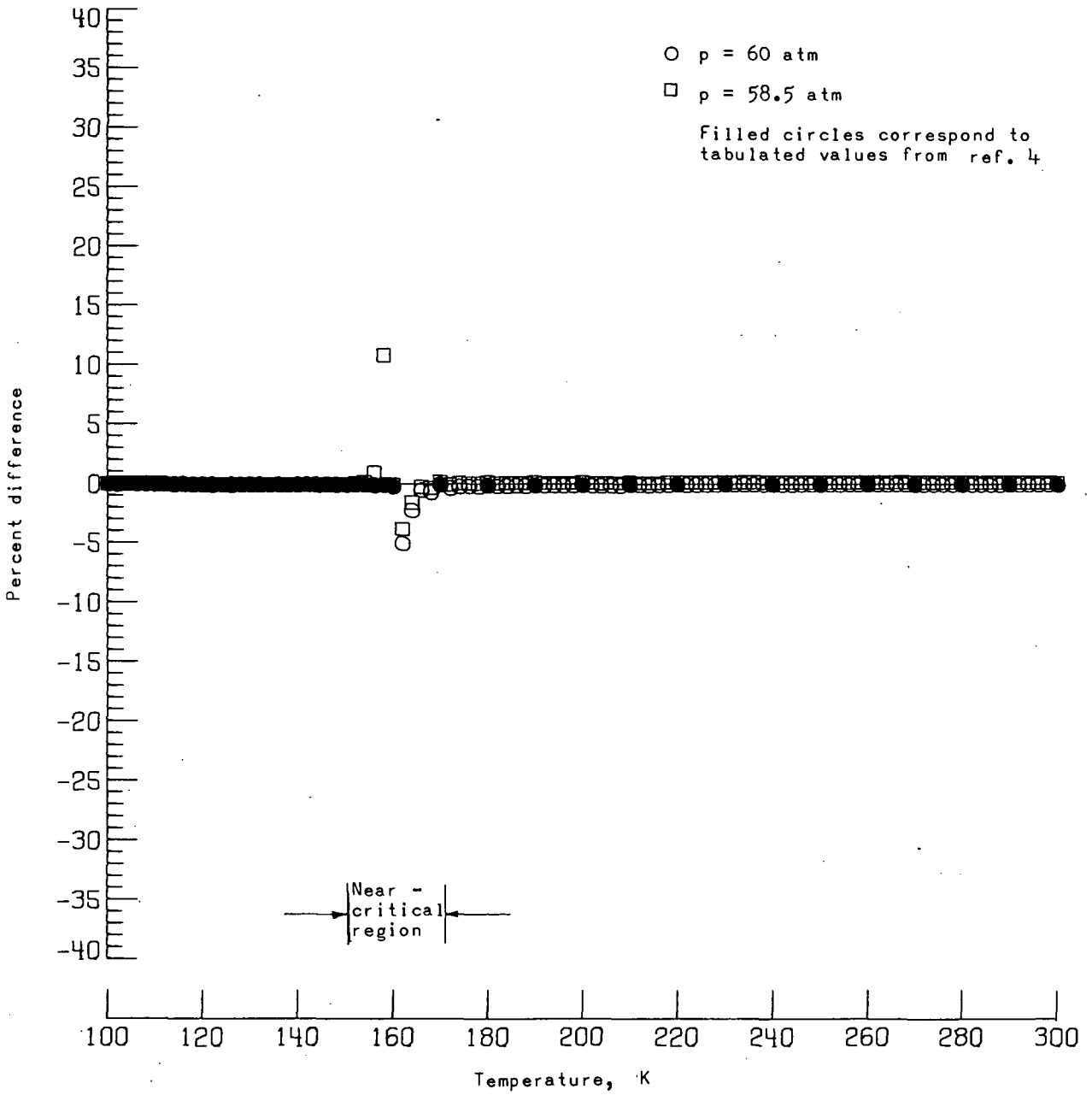

(d) Isotherm derivative $\left(\frac{\partial p}{\partial \rho}\right)_T$.

Figure 1.- Concluded.

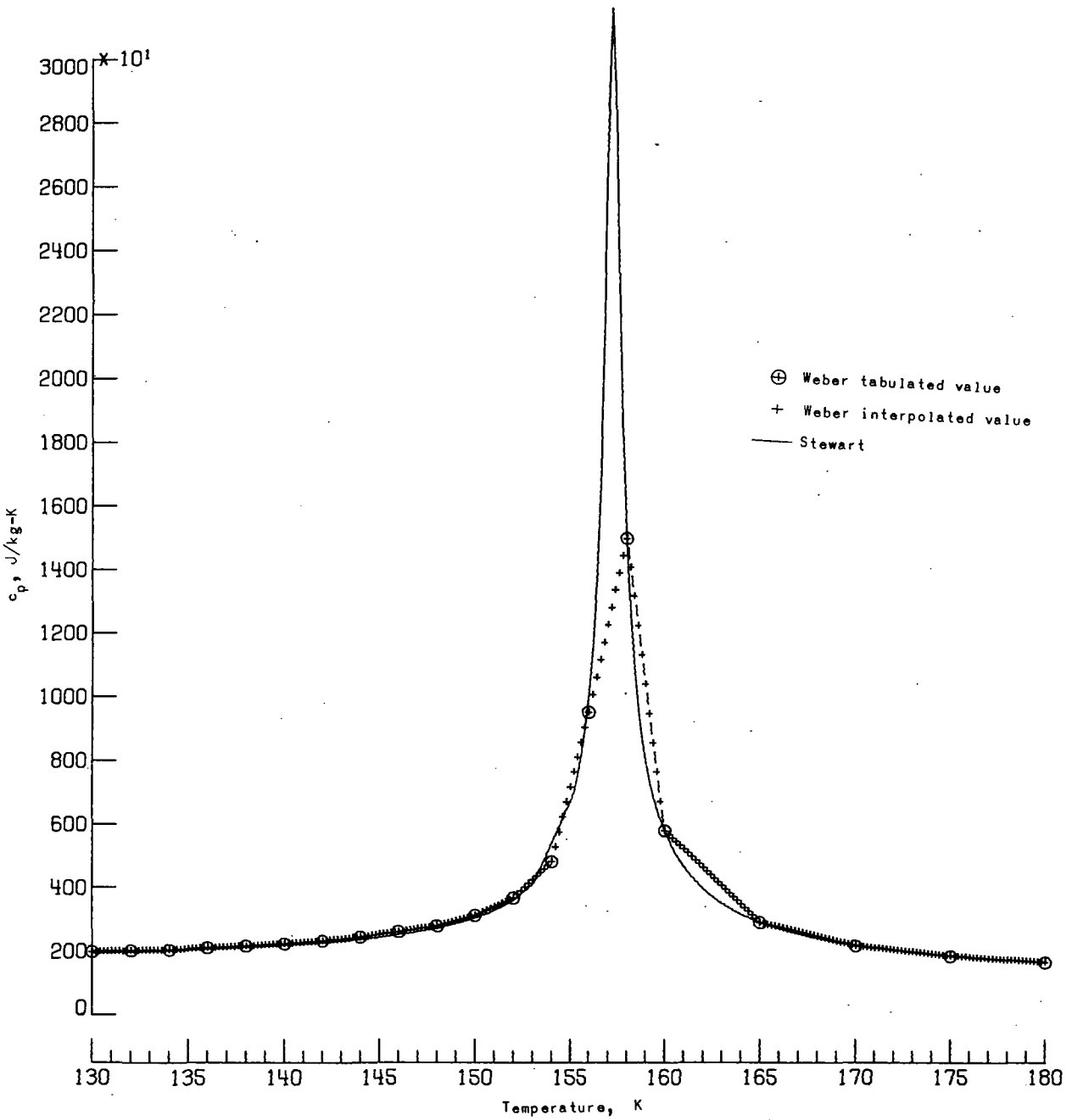

(a) p = 55 atm.

Figure 2.- Comparison of specific heat at constant pressure along selected isobars.

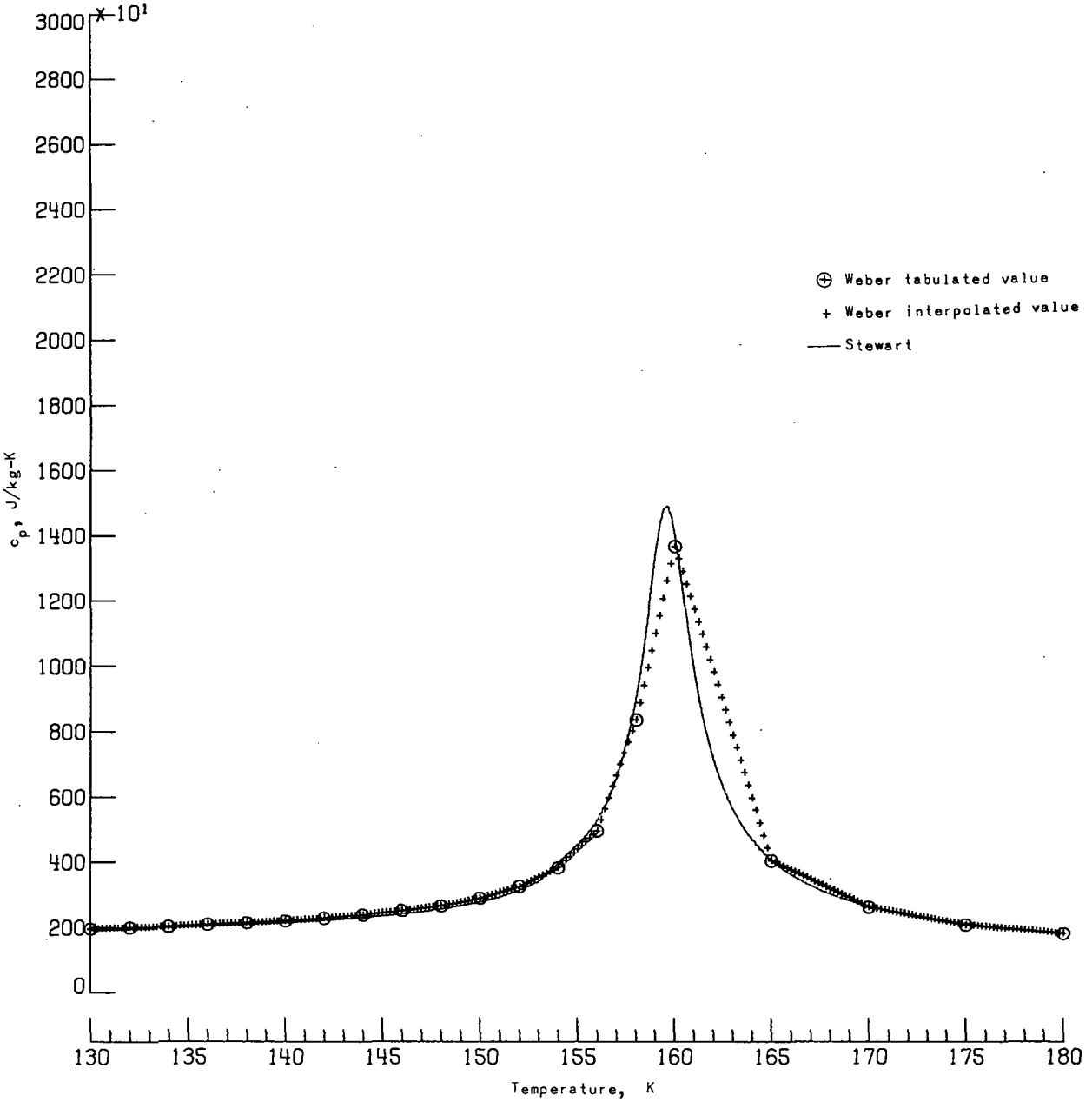

(b) p = 60 atm.

Figure 2.- Continued.

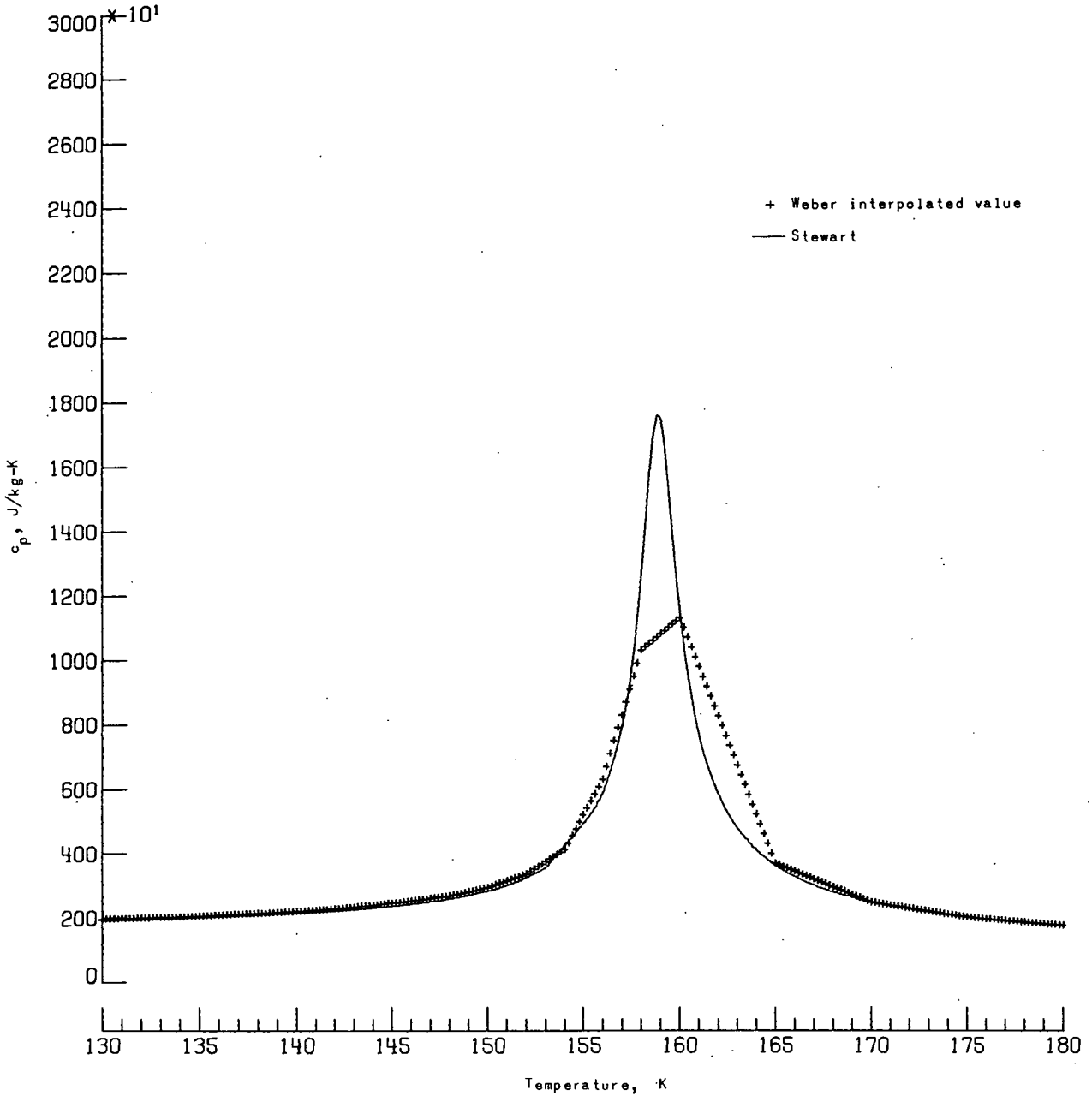

(c) p = 58.5 atm.

Figure 2.- Concluded.

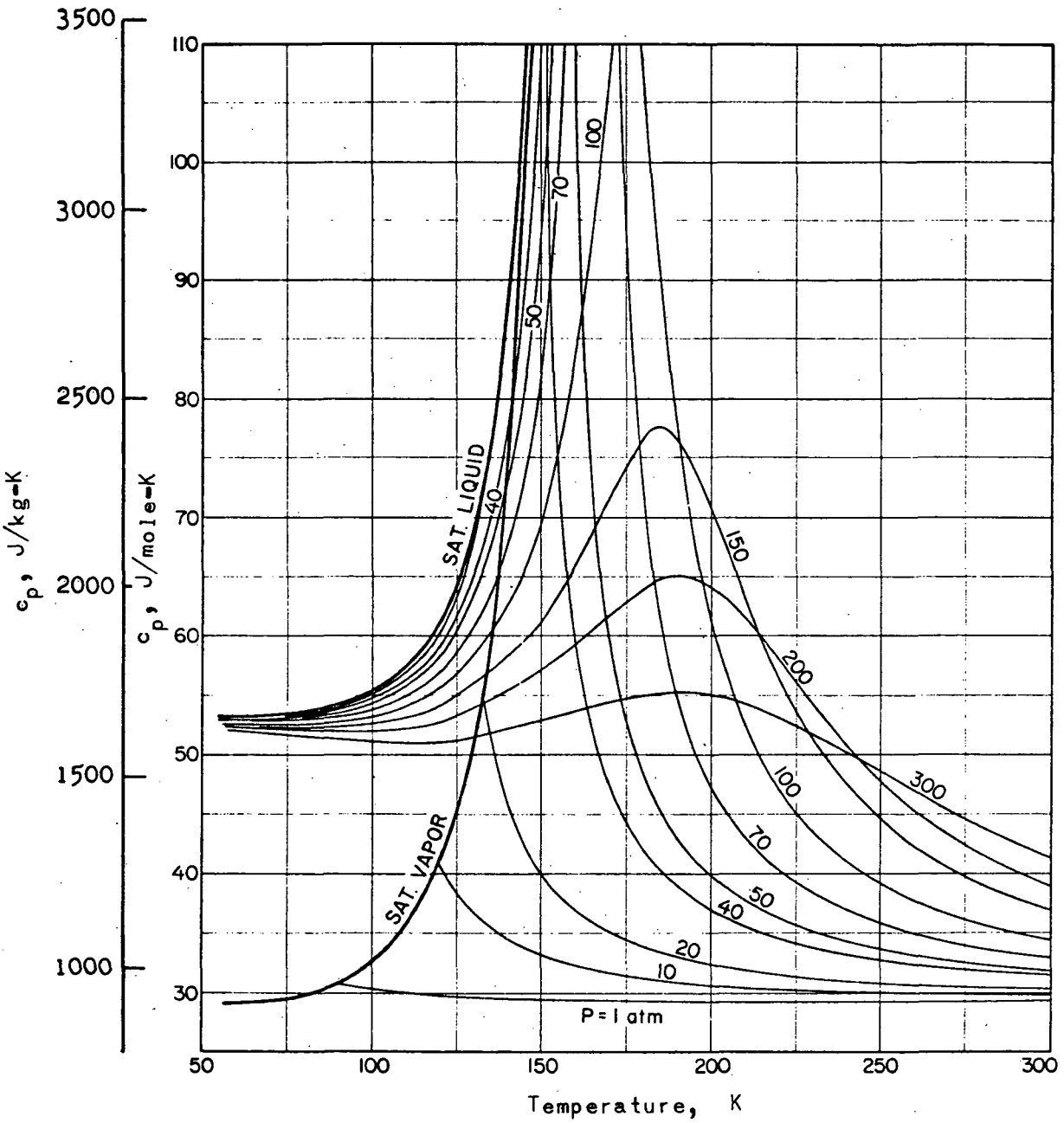

Figure 3.- c_p along selected isobars (ref. 4).

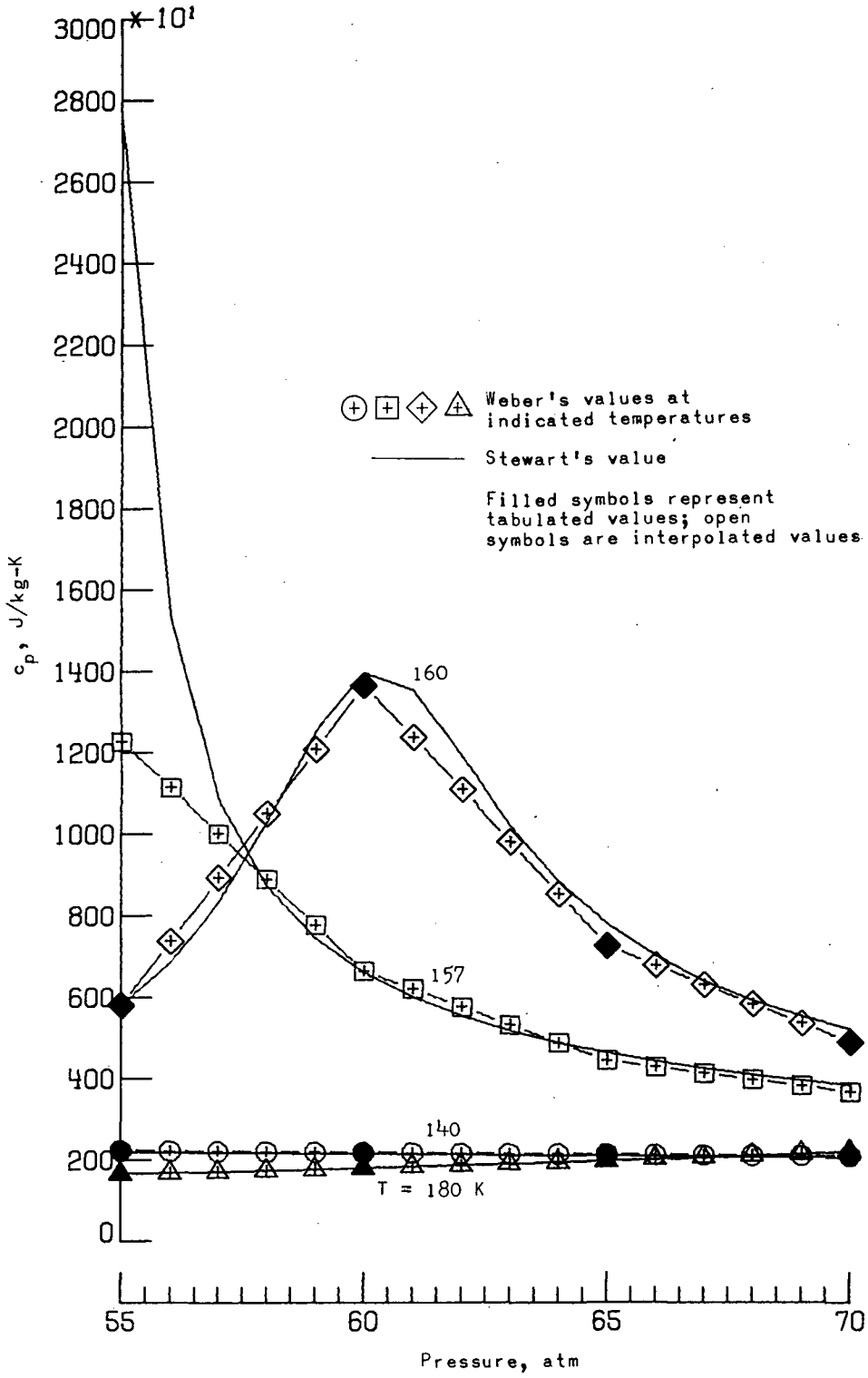

Figure 4.- Comparison of specific heats at constant pressure along selected isotherms.

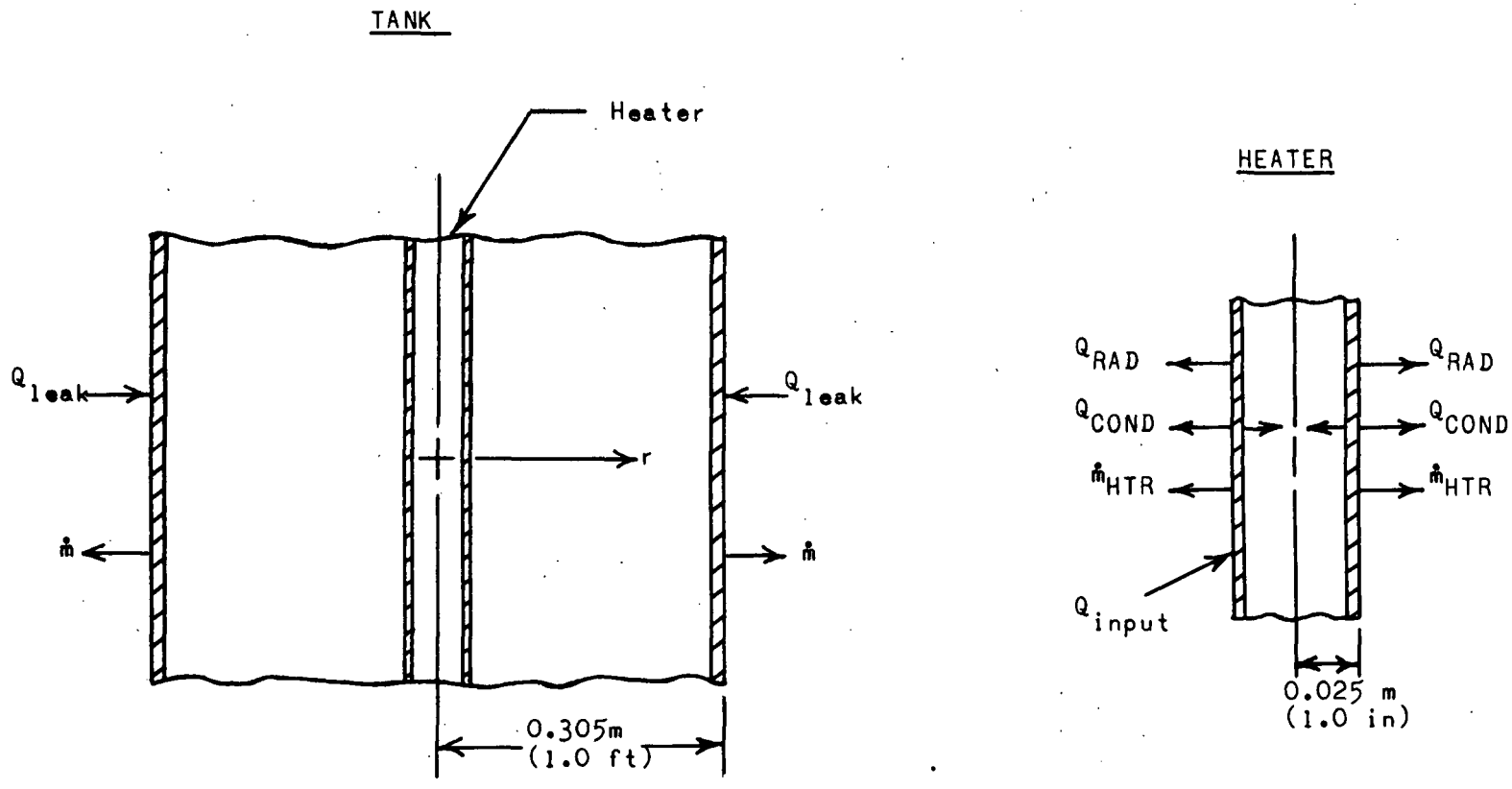

Figure 5.- Sketch of tank and heater showing essential features of model.

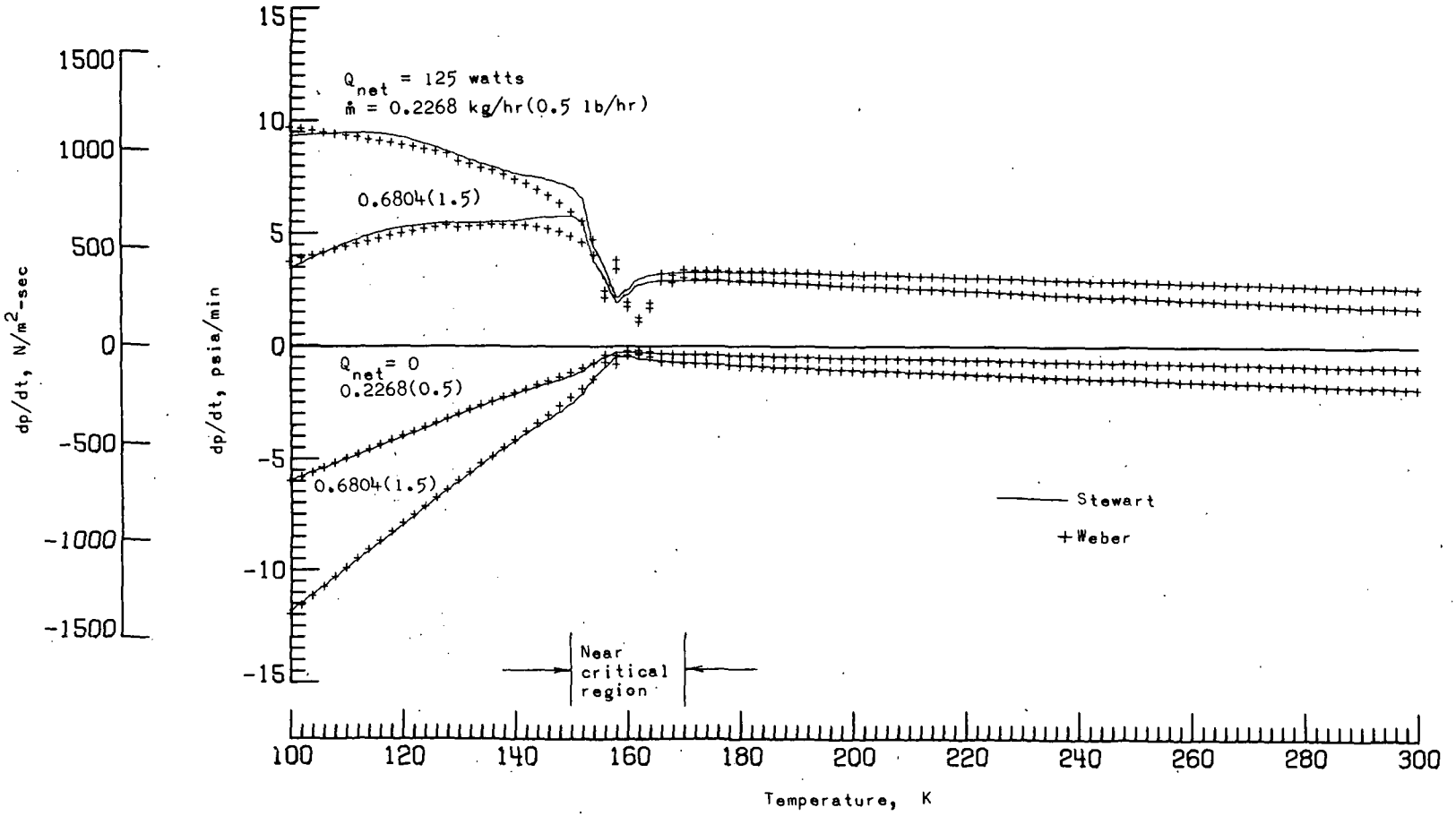

(a) p = 60 atm, a pressure tabulated by Weber.

Figure 6.- Comparison of uniform-tank calculations using Stewart's and Weber's thermodynamic properties.

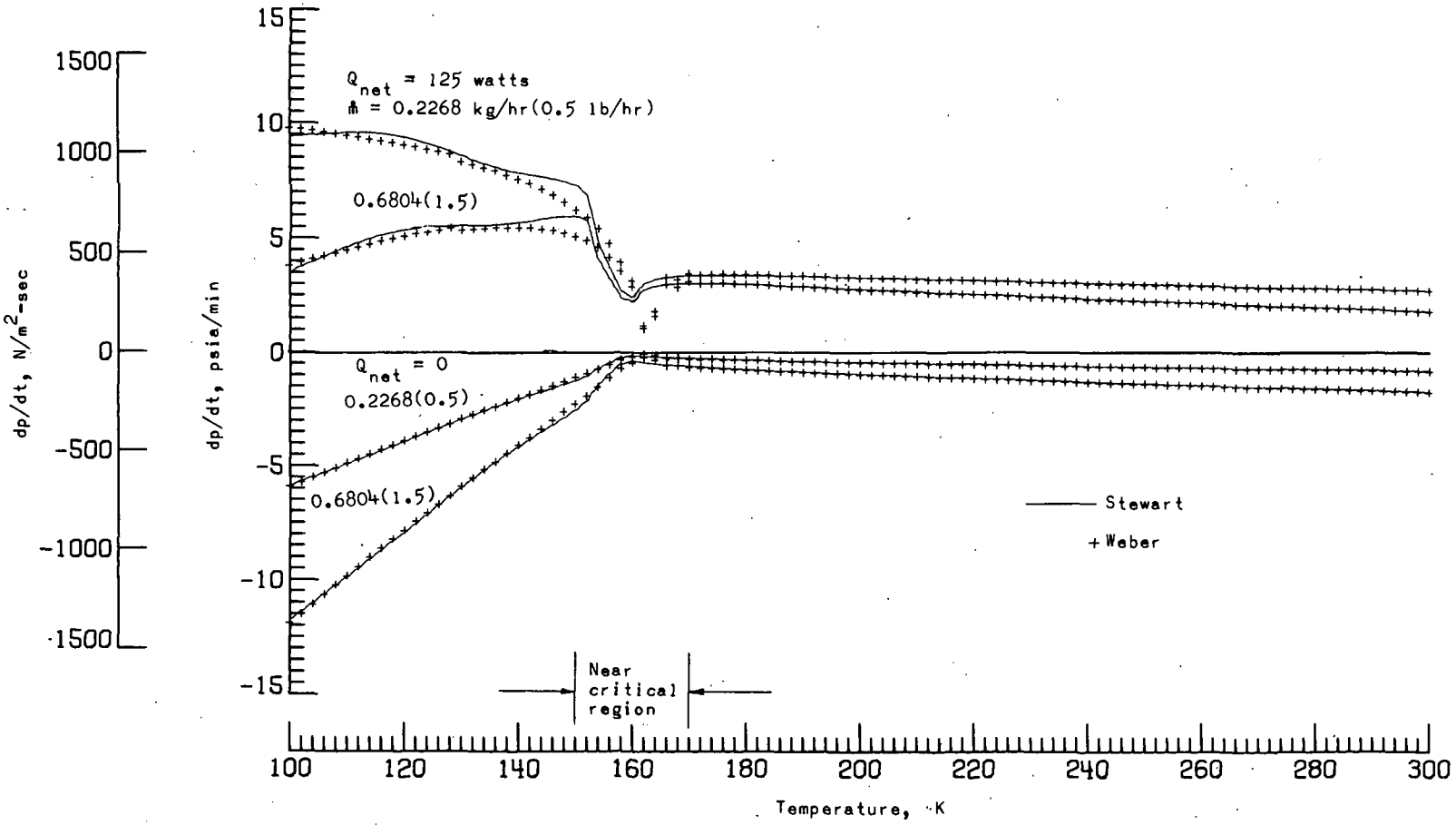

(b) p = 58.5 atm (860 psia) a pressure requiring interpolation in Weber's tabulation.

Figure 6.- Concluded.

"The aeronautical and space activities of the United States shall be conducted so as to contribute . . . to the expansion of human knowledge of phenomena in the atmosphere and space. The Administration shall provide for the widest practicable and appropriate dissemination of information concerning its activities and the results thereof."

—NATIONAL AERONAUTICS AND SPACE ACT OF 1958

NASA SCIENTIFIC AND TECHNICAL PUBLICATIONS

TECHNICAL REPORTS: Scientific and technical information considered important, complete, and a lasting contribution to existing knowledge.

TECHNICAL NOTES: Information less broad in scope but nevertheless of importance as a contribution to existing knowledge.

TECHNICAL MEMORANDUMS: Information receiving limited distribution because of preliminary data, security classification, or other reasons.

CONTRACTOR REPORTS: Scientific and technical information generated under a NASA contract or grant and considered an important contribution to existing knowledge.

TECHNICAL TRANSLATIONS: Information published in a foreign language considered to merit NASA distribution in English.

SPECIAL PUBLICATIONS: Information derived from or of value to NASA activities. Publications include conference proceedings, monographs, data compilations, handbooks, sourcebooks, and special bibliographies.

TECHNOLOGY UTILIZATION PUBLICATIONS: Information on technology used by NASA that may be of particular interest in commercial and other non-aerospace applications. Publications include Tech Briefs, Technology Utilization Reports and Technology Surveys.

Details on the availability of these publications may be obtained from:

SCIENTIFIC AND TECHNICAL INFORMATION OFFICE

NATIONAL AERONAUTICS AND SPACE ADMINISTRATION

Washington, D.C. 20546